EUR 4498 e

COMMISSION OF THE EUROPEAN COMMUNITIES

STUDY OF THE NEUTRON STREAMING THROUGH CYLINDRICAL DUCTS WITH TWO BENDS IN WATER : EXPERIMENTS

Final Report

by

B. CHINAGLIA, G. BOSIO and D. MONTI
(SORIN)

1970

Report prepared by SORIN
Società Ricerche Impianti Nucleari, Saluggia - Italy
Euratom Contract No. 077-66-1 TEEI

LEGAL NOTICE

This report is on sale at the addresses listed on cover page 4

at the price of FF 9.45	FB 85.—	DM 6.20	Lit. 1,060.—	Fl. 6.20

When ordering, please quote the EUR number and the title, which are indicated on the cover of each report.

Printed by Vanmelle, Gand
Luxembourg, September 1970

EUR 4498 e

STUDY OF THE NEUTRON STREAMING THROUGH CYLINDRICAL DUCTS WITH TWO BENDS IN WATER : EXPERIMENTS — Final report
by B. CHINAGLIA, G. BOSIO and D. MONTI (SORIN)

Commission of the European Communities
Report prepared by SORIN — Società Ricerche Impianti Nucleari Saluggia (Italy)
Euratom Contract No. 077-66-1 TEEI
Luxembourg, September 1970 — 62 Pages — 16 Figures — FB 85.—

The problem of neutron streaming through cylindrical bent ducts in water has been studied with a set of experiments in which both the angle and the diameter have been changed (four values for the angle from 15 to 90° and two values for the diameter : 15 and 30 cm).

The results expressed as reaction rates for threshold neutron detectors and thermal and epithermal flux are presented in tables and graphs. They will serve as a basis for future development of calculation procedures.

EUR 4498 e

STUDY OF THE NEUTRON STREAMING THROUGH CYLINDRICAL DUCTS WITH TWO BENDS IN WATER : EXPERIMENTS — Final report
by B. CHINAGLIA, G. BOSIO and D. MONTI (SORIN)

Commission of the European Communities
Report prepared by SORIN — Società Ricerche Impianti Nucleari Saluggia (Italy)
Euratom Contract No. 077-66-1 TEEI
Luxembourg, September 1970 — 62 Pages — 16 Figures — FB 85.—

The problem of neutron streaming through cylindrical bent ducts in water has been studied with a set of experiments in which both the angle and the diameter have been changed (four values for the angle from 15 to 90° and two values for the diameter : 15 and 30 cm).

The results expressed as reaction rates for threshold neutron detectors and thermal and epithermal flux are presented in tables and graphs. They will serve as a basis for future development of calculation procedures.

EUR 4498 e

STUDY OF THE NEUTRON STREAMING THROUGH CYLINDRICAL DUCTS WITH TWO BENDS IN WATER : EXPERIMENTS — Final report
by B. CHINAGLIA, G. BOSIO and D. MONTI (SORIN)

Commission of the European Communities
Report prepared by SORIN — Società Ricerche Impianti Nucleari Saluggia (Italy)
Euratom Contract No. 077-66-1 TEEI
Luxembourg, September 1970 — 62 Pages — 16 Figures — FB 85.—

The problem of neutron streaming through cylindrical bent ducts in water has been studied with a set of experiments in which both the angle and the diameter have been changed (four values for the angle from 15 to 90° and two values for the diameter : 15 and 30 cm).

The results expressed as reaction rates for threshold neutron detectors and thermal and epithermal flux are presented in tables and graphs. They will serve as a basis for future development of calculation procedures.

EUR 4498 e

COMMISSION OF THE EUROPEAN COMMUNITIES

STUDY OF THE NEUTRON STREAMING THROUGH CYLINDRICAL DUCTS WITH TWO BENDS IN WATER : EXPERIMENTS

Final Report

by

B. CHINAGLIA, G. BOSIO and D. MONTI
(SORIN)

1970

Report prepared by SORIN
Società Ricerche Impianti Nucleari, Saluggia - Italy
Euratom Contract No. 077-66-1 TEEI

SUMMARY

The problem of neutron streaming through cylindrical bent ducts in water has been studied with a set of experiments in which both the angle and the diameter have been changed (four values for the angle from 15 to 90° and two values for the diameter : 15 and 30 cm).

The results expressed as reaction rates for threshold neutron detectors and thermal and epithermal flux are presented in tables and graphs. They will serve as a basis for future development of calculation procedures.

KEYWORDS

NEUTRONS
COOLANT LOOPS
WATER
BACKGROUND
RADIATION DETECTORS
THERMAL NEUTRONS
EPITHERMAL NEUTRONS

Index

1. Introduction *)

The shield of a nuclear reactor is always pierced by channels and often the overall performance of the shield system is determined by the streaming through voids and ducts. This is true not only for gas cooled power reactors, but applies also to water cooled reactors, if one considers, for instance, the annular gap around the pressure vessel or the voids existing around the coolant channels. However, in spite of all the work done on neutron streaming, the problem of predicting the neutron flux inside the void and in the medium around the void, cannot be considered as fully resolved.

The shield designer must often decide whether to use analytical approximations (which may be very uncertain) or straightforward general purpose Monte Carlo methods, which usually require very long computing times.

The situation may be much improved by the use of the albedo concept, in conjunction with a Monte Carlo process which describes the individual histories of neutrons reflected along the walls, or alternatively with a simpler iterative (analytical) technique.

Such calculations however have several degrees of complexity and it is very important to know for any particular situation what kind of complexity is required in order to obtain results with a given accuracy. If, for instance, the albedo concept is adopted, the reflection coefficient depends on as many as five variables, three defining the angle of incidence and emission and two the energy of the in-going and out-going particle; considerable saving of computing time may be achieved if the number of variables can be reduced or if simple analytical

---

Manuscript received on 17 April 1970

forms may be introduced as approximations of the true functions describing the wanted dependence.

From these considerations emerges the importance of having a set of experimental data measured in known conditions; these data may serve a dual purpose: to provide a basis for testing the calculations performed with increasing complexity until a sufficient accuracy is reached and to permit, when possible, an empirical correlation between some relevant quantities (such as the neutron flux on the axis in the case of a cylindrical duct) and various geometric parameters.

Since some years a cooperation exists between SORIN and CCR Euratom-Ispra for the research on the neutron streaming problem following a development program of experiments and calculations according to the line described above. A part of the work has been performed previously under an Euratom contract for the study of the neutron penetration in straight cylindrical ducts in water /1/ and a second part concerning experiments on cylindrical ducts with two bends is the object of the Contract 077-66-1-TEEI. This report describes the results obtained under this Contract and therefore contains only the experimental data.

These have been already published in the three-monthly progress reports and in the first annual report /2/, furthermore some results and the details of some calculation procedures have been the object of a common paper SORIN - CCR Ispra /3/.

2. Experiments

It was considered very important to know the effect of a

bend on the spatial and energy distribution of neutrons. Therefore 4 values of the angle between straight sections (15°, 30°, 60°, 90°) have been examined for 2 duct diameters (15 and 30 cm). Furthermore the neutron spectrum determination requires at least 4 different detectors: one for thermal neutrons, one for epithermal neutrons, and two (having a low and high threshold) for fast neutrons.

The choice of the detectors depends on the sensitivity and on possible errors deriving from parasitic effects.

Activation foils represent the best solution for a detailed spatial measurements; for thermal and epithermal neutrons there is no serious difficulty and the reactions $Dy(n,\gamma)$ and $Au(n,\gamma)$ have been used. For fast neutrons there are some limitations and in some cases only detectors with intermediate threshold energy (~4 MeV) may give reliable results. This limitation derives from two effects:

- Possible low threshold (~1 MeV) reactions are $In(n,n')$ $Rh(n,n')$, $Np(n,f)$; in all cases there is a spurious contribution to the activation due to (γ,γ') or (γ,f) reactions. When the distance from the source is small the neutron to gamma flux ratio is such that the contribution is negligible and no correction is needed; in some ducts however after the bend the neutron flux falls off very rapidly with respect to the γ flux and the photo-activation is predominant. In these cases the results are no more reliable and there is no possibility to correct for the spurios contribution with a sufficient degree of approximation. Reactions with high threshold energy such as $Al(n,\alpha)$ have a low sensitivity and, taking into account the source power, it is not possible to

measure attenuations beyond 10^{-4}.

For these reasons in many cases the fast neutron flux has been measured beyond a given distance only with S(n,p) or P(n,p) detectors, which possess an intermediate threshold energy but are not affected by spurious reactions and have a rather high cross section.

2.1 - The irradiation facility

The irradiation facility is the ETNA lid tank shown in Fig. 1 and 2 and described in detail in previous report /1/.

During the course of the experiments the working conditions were the following:

- source: natural uranium, thickness 2 cm, diameter 90 cm
- reactor power: (5 + 7) MW
- Materials between source and water: boral slab (1/4"); 19 cm air; 4 cm Al (wall of the tank)

With respect to the previous work /1/ the reactor power has been increased; however also the core configuration and its distance from the thermal column have been changed, so that the actual source power at 5 Mw is now slightly lower than previously at 2 Mw.

However all the experimental data are always normalized to the same thermal flux impinging on the source, and therefore to the same source power.

This latter has been calculated with two methods: from the thermal flux on the source and from the fast flux at the input of the tank. In the first case the hypothesis has been made that the thermal flux inside the uranium slab decreases exponentially. From the values before and after the slab

and along a radius of the source, the thermal flux inside the source can be described by:

$$\varphi(r,z) = 2,3\cdot10^{8}(1- 5,6\cdot10^{-6}r^{2} - 1,4\cdot10^{-8}r^{4})e^{-0,585\cdot z}\ n/cm^{2}s \qquad (1)$$

where r and z are the radial and axial coordinates in cm and an absolute error of 5% is estimated.

The mean number of fissions per unit volume in the source is given by:

$$n_f = \frac{\Sigma}{R^2}\int_0^R\int_0^{z'}\varphi(r,z)\,r\,dr\,dz = (2,65 \pm 0,15)\cdot10^{7}\ \text{fission}/cm^{3}\cdot s \qquad (2)$$

where $R = 45$ cm, $z' = 2$ cm and $\Sigma = 0,20\ cm^{-1}$ is the macroscopic fission cross section for natural uranium.

In the second case whe have used the values of the reaction rates for Ni(n,p) and Al(n,α) (see below Table I) measured at the input of the water tank.

These values can be calculated by:

$$R.R. = 2.44\cdot N\int_E\int_V \frac{n_f(V)K(\varrho',E)}{\varrho^2}\,dV\cdot\sigma(E) \qquad (3)$$

where:

RR = reaction rate per gram element

$\sigma(E)$ = activation cross section

N = number of atoms of the isotope in consideration per gram element

$n_f(V)$ = fission rate per unit volume in the volume dV

ϱ = distance between dV and measuring point

ρ' = equivalent water thickness crossed by the ray along ρ (actually U and Al are crossed, and the equivalent thickness is calculated as the actual thickness multiplied by the ratio of the material removal cross section to the water removal cross section ; $\Sigma'_{H_2O} = 0,103\ cm^{-1}$).

$K(\rho' E)$ = attenuation Kernel derived from the moments method calculation in water [4].

E = neutron energy

With the values of Table I it has been deduced that the source must be:

$$n_f = (2,9 \pm 0,4) \cdot 10^7 \quad \text{fission/cm}^3\ \text{s}$$

in good agreement with the previous one. The mean value may therefore be taken as

$$n_f = (2,7 \pm 0,1) \cdot 10^7 \ \text{fission/cm}^3\text{s}.$$

From this the following quantities are deduced:

- power per unit volume: $0,87 \cdot m$ watt/cm^3
- totale power: 11 watt

The activations (or flux in the case of thermal neutrons) deriving from this source in the tank are shown in Table I and II.

Table I refers to a measuring point on the axis of a 30 cm diameter duct at $z = o$ (see Fig. 1); for a 15 cm diameter duct fast activations are the same within experimental errors (order of 5%), epithermal and thermal flux are about 30% higher.

Table II refers to measuring points in water (without duct) on the axis of the source as a function of the water distance z.

The neutron spectrum at the input of the tank has a shape slightly different from a fission one, due to energy losses in scattering process within the source and Al wall and reflections from walls; the actual shape has been derived by an analysis of the data of Table I and the result is shown in Fig. 3; this spectrum modification does not seem to have any sensible influence on the attenuation in the ducts and for calculation purposes the spectrum can be considered a fission one.

2.2 - Duct configurations

The duct material is Vedril (C 60%, O 32%, H 8%) which can be considered equivalent to water as far as the nuclear properties are considered.

During the irradiation the axis of the first section is coincident with the source axis, as shown in Fig. 1.

Each configuration is characterized by the inner diameter, the length of the first, second and third straight section, and the bend angle. Therefore the configuration of Fig. 1 is indicated as $(d, l_1, l_2, l_3; \alpha)$ where d and l_i are in cm, α in degrees. Also shown in Fig. 1 is the coordinate system used to define the measurement point: z is the distance along the axis measured from the mouth. Also shown in Fig. 1 are the coordinates z_1, z_2 and z_3 with origin at $z = 0$, $z = l_1 + \Delta z$ and $z = l_2 + \Delta z$, where $\Delta z = d/2 \sin \alpha$; they define the distance on the axis in

each section measured from the intersection with the preceeding section. The complete list of the configurations with the geometric parameters and the measurements performed is shown in Table III: the first one (T) is a test configuration which does not fit the scheme of the other ones; config. 1a and 1b differ for the thickness of the wall on the mouth which is 2 cm for 1a and 0,30 cm for 1b ÷ 10; conf. 9 and 10 are the same as 6 and 2, but with the first leg extendend beyond the bend in order to acquire information on the contributions of different parts of the bend on the reflection. The cylindrical wall thickness is always 0,5 mm and the material composition C 60%, O 32%, H 8%.

The last configuration (G) refers to the gap around the tank; as shown in Fig. 2 between the aluminum wall of the tank and the concrete shield there is an air gap of 20 cm thickness, 3 m wide, which acts as a streaming path in parallel with the ducts.

Measurements in this gap have been performed in order to correct for this spurious contribution the data at the end of the ducts.

2.3 - Detectors

The criteria followed for the choice of detectors has already been explained.

A particular difficulty found in this work has been the problem of detecting in a single experiments activities in a wide range, with lower limits below the background of usual counters.

The sensitivity limits have been improved by increasing

the size of the detectors at strong attenuations, and by the use of counters of low background and large sensitive volume prepared for the various specific applications together with other techniques such as burning sulphur pellets at 370°C for the separation of P^{32} activity as described in ref. 5.

Counters of different sensitivity and detectors of different size have been intercalibrated in order to obtain in each experiment normalized counting rates relative to a standard detector size. The counting rates are then processed according to standard methods to give, when it is necessary, reaction rates (i.e. saturation absolute activities) per gram element or flux.

The list of the detectors is shown in Table IV together with the method of counting and of standardization. For most γ-ray emitting nuclides the standardization is based on the use of a calibrated detector [6]. Some of the detectors have been used only for measuring the flux shape at the mouth, in which case it was considered important to have a large number of reactions for permitting the analysis of Fig. 3.

Among these detectors there are the fission chambers coated with Np, Pu. The method used to standardize the chambers is described in some detail in the Appendix.

3. Results

The results of the measurements on the axis are presented in Tables V to XVI and in Fig. 4 to 14. All the data are normalized to the input value (see Table I); the relative er-

ror arising from statistical uncertainties is reported in Tables and graphs when it is greater than 2%. Vertical lines have been drawn in the figures at $z = l_1 + \Delta z$ and $l_2 + \Delta z$; it is clearly seen that at these points all the curves giving the flux as a function of z show a more or less marked change in slope, corresponding to the loss of total visibility of the preceeding section. A boral or Cd disk, unless otherwise specified, has always been placed at the end of the ducts to reduce the thermal neutron reflection. Also the values measured at the end have been corrected for the spurious contribution deriving from the gap around the tank; this contribution has been measured by irradiating only the last section of a duct as shown in the insert of Fig. 13. In Fig. 13 are also shown the curves of neutron flux and gamma dose attenuation along the gap or in water near the tank wall (at 3 cm from the aluminum wall).

For completeness other results obtained with Cd foils in particular positions are presented in Fig. 14, 15 and 16. In the first two straight Al ducts have been considered, diameter 30 and 10 cm. All the duct was covered with Cd (thickness 0,02 cm) with the exception of a cylindrical window extending from $z-\varepsilon$ to $z+\varepsilon$ (the actual value of ε ranged from 1 cm to 5 cm according to the value of z). In Fig. 14 or 15 are shown the following quantities:

- the thermal flux on the axis measured with Dy without any window, this represents the background and is not actually a thermal flux, but rather the epicadmium activation of Dy expressed in thermal flux units
- the thermal flux on the axis subtracted from the above back

ground, measured with windows of size specified in the figures at various Z.

From this experiment a very important quantity is derived, i.e. the thermal neutron current entering the duct walls. The analysis of these data has been performed by assuming a cosine distribution of the current; this is in fact confirmed by the agreement of experimental points and a curve giving the flux on the axis with the above hypothesis, at least in the range where experimental errors permit a comparison, as shown in Fig. and 14 and 15. In this case the flux on the axis at $Z = Z_W$ is given by:

$$\phi (Z_W) = \frac{4\varepsilon}{a} \cdot i(Z_W)$$

where a is the duct radius, and i(Z) the current deriving from the unreflected current $i^o(Z)$ and the current reflected by the walls.

The reflection is possible only within $Z_W - \varepsilon$ and $Z_W + \varepsilon$ and a simple relationship between $i^o(Z)$ and i(Z) is:

$$i(Z) = i^o(Z) \cdot \frac{1}{1 - \alpha \cdot \varepsilon}$$

where for α (the albedo) the value 0,8 has been used. The initial or unreflected current $i^o(Z)$ determined by this method is reported in Tab. XVII.

Fig. 16 refers to a bent duct (conf. 5) in which the thermal flux (actually Dy counting rate) has been measured after the insertion of a Cd shutter in various position as shown in the insert. The results of this experiment show that the thermal

neutron flux at the end of the duct is deriving for ~60% from neutrons which enter the bend volume at thermal energies, for ~20% from neutrons which become thermal in the bend. An important consequence of this result is that any calculation which does not take account of energy degradation at the bend will be in error of about a factor 2.

4. Conclusions

The reported values of neutron streaming through bent ducts represent a detailed, although not complete, serie of data describing the spatial and energy distribution of flux.

The limits of this work are mainly two:

- The sensitivity of detectors or the spurious contributions in some cases do not permit the measurement along all the duct. However this is not very important because from a realistic point of view when the attenuation is very high there is no or little interest in the prediction of the streaming flux. This is the case of high threshold energy detectors whose activity falls off after the bend very rapidly with respect to the thermal and epithermal flux, and this means that the contribution of the high energy neutrons to the total dose streaming after the bend is negligible.
- The geometric parameter (duct radius) has not been examined in a wide range. In particular no information has been obtained for radii small compared with neutron relaxation lengths where the reflection dependence on the duct radius is expected to be important. The examined radii are however in the order of sizes existing in a reactor shield and the main interest lies in this range of sizes.

Attempts to correlate the experimental data with a semiempirical formula have given a very poor agreement and a limited range of validity; in particular the Simon-Clifford formula applied to thermal or epithermal neutrons does not fit adequately our results and this is partly due to the approximations in the formula, and partly to the quite different source conditions. The source in our experiments emits no thermal or epithermal neutrons, and the energy degradation along the duct cannot be neglected, as could be the case for different source spectra. The absence of the direct thermal and epithermal flux from the source permits a comparison with calculations of the energy degradation more significant than previous experiments.

Some details of calculation performed by R. Nicks (Monte Carlo, last collision) have been reported elsewhere; for thermal and epithermal neutron the approach of the problem with the albedo concept is expected to be the most reliable and simple method and results already obtained for straight ducts together with the information gained with this work indicate that few energy groups are needed. Calculation work according to this line is now in progress and will be reported elsewhere.

Appendix

Calibration of fission chambers

The counting rate C of a fission chamber is given by:

$$C = \varepsilon p F$$

where F is the fission rate per unit mass of the fissile element, p the weight of the fissile element, and ε the probability that a fission event gives a detected count.

For plane fission chambers and very thin coatings $\varepsilon \sim 1$, but for cylindrical chambers and rather thick coatings as in our case $\varepsilon < 1$, the exact value depending also on the electronic chain. The weight p is given by the manufacturer but it can be considered only a nominal value. The problem is therefore to determine the product (εp).

Pu^{239}

In this case there is a strong activation cross section in the thermal energy. An irradiation in a known thermal flux gives the value of (εp) as the ratio C/F_{th} where

$$F_{th} = \sum \Phi_i \sigma_i \cdot \frac{6 \cdot 10^{23}}{240}$$

and Φ_i, σ_i are group fluxes and cross section below the cadmium cut off. These have been calculated with removal diffusion (Sabine) in water and the normalisation to the absolute value has been obtained with gold irradiated around the chamber. Epi thermal contribution have been subtracted with a second irradiation with cadmium (cut off 0,5 eV for 2 mm Cd).

At the duct mouth from the measured counting rate we obtain:

$$F = 1,3 \cdot 10^{6} s^{-1} g^{-1} \quad (E_n > 0,5 \text{ eV})$$

U^{238}

The chamber has been irradiated together with a foil of depleted U(350 ppm). From the La^{140} activity in the foil, corrected for the residual epithermal activity from U^{235}, we obtain at the duct mouth $F = 3,7 \cdot 10^4\ s^{-1}g^{-1}$ and the ratio C/F assuming a value of 0,057 for the Ba^{140} yeld. The weight p of U in the chamber has been determined in a separate experiment by measuring the activity of U^{239} of the chamber and of a standard by the usual methods of activation analysis. From these values one obtains:

$$\varepsilon = \frac{C}{F \cdot p} = 0,5 \pm 0,1$$

where the main error is due to the assumptions made in the evaluation of the attenuation of U^{239} γ rays in the chamber walls.

Np^{237}

The value of p has been determined by measuring the activity of Pa^{233} of the chamber. We have used the value of 0,44 for the intensity of the 0,313 MeV γ line of Pa^{233} (UCRL 8642).

For ε the value $0,5 \pm 0,1$ previously found for U has been adopted.

From the measured counting rate it results at the duct mouth:

$$F = (2,2 \pm 0,4) \cdot 10^5\ s^{-1}g^{-1}.$$

References

/1/ B. Chinaglia, D. Monti "Studio delle irregolarità nelle schermature" - Rapporto finale SORIN F/326 (1964)

/2/ B. Chinaglia, G. Bosio, D. Monti "Studio della propagazione neutronica in condotti tubolari con 2 gomiti" - Rapporti F/414, F/433, F/455, F/478, F/508, F/510, F/515, F/526 (1966 ÷ 1968)

/3/ U. Canali, B. Chinaglia, D. Monti, R. Nicks "Neutron propagation through cylindrical ducts" - AERE R/5773, p. 657 (1968)

/4/ D.K. Trubey - ORNL 3487 (1964)

/5/ D.C. Santry, J.P. Butler - Can. J. of Chemistry, 41, n. 1, p. 123, (1963)

/6/ B. Chinaglia, R. Malvano - Nucl. Instr. & Methods 45, p. 125, (1966)

TABLE I

Reaction rates per gram element and gamma flux measured at the mouth of a duct of 30 cm diameter. (a)

Reaction	Reaction Rate $[s^{-1}\ g^{-1}]$	
$Au^{197}(n,\gamma)$ thermal	$6,61 \cdot 10^{6}$	$\pm$ 3%
$Au^{197}(n,\gamma)$ epithermal	$5,09 \cdot 10^{6}$	"
$S^{32}(n,p)$	$3,07 \cdot 10^{4}$	5%
$Al^{27}(n,p)$	$2,19 \cdot 10^{3}$	"
$Al^{27}(n,\alpha)$	$3,94 \cdot 10^{2}$	"
$In^{115}(n,n')$	$2,87 \cdot 10^{4}$	"
$Pu^{239}(n,f)$	$1,3 \cdot 10^{6}$	10%
$Np^{237}(n,f)$	$2,2 \cdot 10^{5}$	"
$U^{238}(n,f)$	$3,7 \cdot 10^{4}$	"
Gamma dose	400 R/h	5%
Thermal flux (Dy)	$1,68 \cdot 10^{7}$	5%

(a) **Actually the mouth value is measured at:**

Z = (0 ÷ 0,1) cm for Dy, Au, In

Z = 0,2 cm for Al

Z = 0,5 cm for PS

Z = 0,8 cm for γ dose and chambers

TABLE II

Reaction rates per gram element or flux in plain water (without the ducts), as a function of water thickness Z.

Z (cm)	Ni(n,p)	In(n,n')	Au/Cd	Thermal Flux
0	$2.02 \cdot 10^{4}$	$1.4 \cdot 10^{4}$	$1.12 \cdot 10^{7}$	$1.68 \cdot 10^{7}$
4	$8.8 \cdot 10^{3}$	$4.6 \cdot 10^{3}$	1.22 "	8.2 "
8	4.5 "	2.15 "	$5.45 \cdot 10^{6}$	5.8 "
12	2.35 "	1.02 "	1.98 "	2.8
16	1.25 "	$5.25 \cdot 10^{2}$	$8.0 \cdot 10^{5}$	1.3 "
20	$6.7 \cdot 10^{2}$	2.75 "	3.52 "	$5.8 \cdot 10^{6}$
24	3.8 "	1.48 "	1.63 "	2.6 "
28	2.02 "	$8.2 \cdot 10^{1}$	$8.2 \cdot 10^{4}$	1.19 "
32	1.13 "	4.52 "	4.1 "	$5.75 \cdot 10^{5}$
36	$6.8 \cdot 10^{1}$	2.59 "	2.08 "	2.9 "
40	3.9 "	1.52 "	1.1 "	1.58 "
44	2.39 "	$8.7 \cdot 10^{0}$	$6.2 \cdot 10^{3}$	$8.45 \cdot 10^{4}$
48	1.39 "	5.3 "	3.5 "	4.5 "
52	$8.3 \cdot 10^{0}$	3.2 "	2.0 "	2.4 "
56	5.0 "	1.9 "	1.13 "	1.38 "
60	2.9 "	1.15 "	$6.5 \cdot 10^{2}$	$7.9 \cdot 10^{3}$
64	1.75 "		3.68 "	4.6 "
68	1.02 "		2.15 "	2.64 "
70	$8.0 \cdot 10^{-1}$		1.57 "	2.03 "
72				1.59 "
74				1.2 "

TABLE III - List of the examined duct configurations

Configuration	d(cm)	l_1(cm)	l_2(cm)	l_3(cm)	ΔZ(cm)	α(°)	Detectors Used
Test configuration	7,1	79,7	102	83	5	45	S(n,p); Dy(n,γ)
1 a	28,7	104,2	82	106	55	15	Dy(n,γ)
1 b	28,7	104,2	82	106	55	15	Dy(n,γ); In(n,n'); P; γ dose
2	28,7	108	104	111	20	45	Dy, Au/Cd; In(n,n'); P; S; Al(n,p); Al(n,α); γdose
3	14,2	98,5	97,5	95,5	27	15	Dy; Au/cd; S; γ dose
4	14,2	96,5	140,5	93,5	10	45	Dy; Au/cd; S; γ dose
5	28,7	107,7	145,7	110	16,5	60	Dy; Au/cd; In(n,n'); S; Al(n,α); γdose
6	28,7	166	127	122	14,3	90	Dy; In(n,γ)/Cd, In(n,n'); P; γ dose
7	14,2	102,3	145	116,3	8,2	60	Dy; Au/cd; In(n,γ)/cd; S; γ dose
8	14,2	142,4	125	147	7,1	90	Dy; γ dose
9	28,7	166 +74	127	122	14,3	90	Dy; P
10	28,7	108 +92	104	111	20	45	Dy; In(n,γ)/Cd; Au/cd; P; S
G	*	140	312	140	10	90	Dy, In(n,γ)/Cd; γ dose

*Rectangular duct (300 x 21) cm^2 (see Fig. 13)

TABLE IV - List of detectors

Detectors	Form *	Counting	Standardization
Au (**)	disk; 0,2 g/cm^2 1,2 cm	β	γ
S	disk; 0,5 cm up to 5 cm	β	4 π- β
Al	disk; 1 + 2 mm 5 cm	γ	γ
In	disk; 0,5 mm up to 5 cm	γ	γ
Al/Dy (10%)	disk; 0,1 cm 1 cm	β	comparison with Au
Chambers FC 4-20th Century	cylind; 2,2 cm 0,63 cm	——	——
γ dose	Dosimeter pen	——	Co^{60}

* For disks: first number thickness
second number diameter

For cylinder: first number length
second number diameter

(**) Correction factor used for flux depression:
- thermal 0,9
- epithermal 0,22

TABLE V - Test configuration (7.1; 79.7; 102; 83; 45°)

Z (cm)	*F(Z) S(n,p)	ε%	F(Z) Dy(n,γ)	ε%
0	1		1	
38	2,3/-2		3,23/-3	
82	1,72/-3	8	4,04/-4	
134	1,35/-4	5	5,65/-6	5
184	1,5/-5	6	1,45/-6	25

*F(Z) = ratio between activation measured at Z and at the mouth (Z = o) in Tables V to XVI.

TABLE VI - Configuration 1a*) (28,7; 104,2; 82; 106; 55; 15°)

Z (cm)	F (Z) Dy (n,γ)
0	1
30,2	0,620
60,5	0,310
80,8	0,193
101,8	0,124
111,8	0,105
135,7	0,062
160,7	0,037
177,3	0,026
190,3	0,020
220,6	0,012
251,1	0,008
271,6	0,006
292,0	0,0068

*thickness of mouth wall: 2 cm.

TABLE VII - Configuration 1b) (28,7; 104,2; 82; 106; 55; 15°)

Z (cm)	F(Z) Dy (n,γ)	ε%	F(Z) In (n,n')	ε%	F(Z) P (n,p)	ε%	F(Z) Dose γ	ε%
0	1		1		1		1	
10	1,032		7,0 /-1					
30	7,5 /-1		2,35/-1		2,35/-1			
40							3,8 /-1	
50	4,72/-1		9,8 /-2		8,7 /-2			
70			4,90/-2					
90	1,90/-1		3,0 /-2		2,80/-2		1,40/-1	
102	1,56/-1		2,4 /-2		2,2 /-2			
110	1,28/-1		2,19/-2		1,82/-2		9,80/-2	
114	1,19/-1		2,0 /-2		1,70/-2		9,0 /-2	
130	8,40/-2		1,60/-2					
140	6,80/-2	1	1,40/-2				5,30/-2	
145	6,10/-2	1	1,35/-2		1,0 /-2			
150			1,25/-2		9,20/-3			
160	4,50/-2	1	1,10/-2					
180	3,00/-2	1	5,80/-3	5	4,49/-3	2	2,40/-2	
190	2,59/-2	1	4,49/-3	10				
200	2,18/-2	2	3,60/-3	10				
210			3,30/-3	5	3,50/-3	3		
220	1,46/-2	2	3,20/-3	10			1,60/-2	2
230			3,0 /-3	5			1,55/-2	3
240			2,80/-3	10	2,80/-3	3		
250			2,65/-3	5				
260	7,50/-3	3	2,50/-3	10				
270			2,38/-3	10				
280	4,40/-3	3	2,20/-3	20			1,15/-2	1(
290	3,10/-3	3	2,10/-3	30	2,10/-3	5		
292			2,06/-3	40				

TABLE VIII - (28,7; 108; 104; 111; 20; 45°)

Z(cm)	F(Z) Dy(n,γ)	ε%	F(Z) I(n,n')	ε%	F(Z) P(n,p)	ε%	F(Z) S(n,p)	ε%	F(Z) Au/cd	ε%	F(Z) Al(n,p)	ε%	F(Z) Al(n,α)	ε%	F(Z) dose γ	ε%
0	1		1		1		1		1		1		1		1	
10	1		7,45/-1		7,22/-1		7,22/-1		7,30/-1		--		--		--	
20	--		--		--		--		--		4,50/-1		4,50/-1		--	
30	--		--		2,53/-1		2,53/-1		4,50/-1		3,10/-1		3,10/-1		4,90/-1	
40	--		--		--		1,60/-1		3,44/-1		2,10/-1		2,10/-1		3,80/-1	
50	4,79/-1		1,04/-1		1,10/-1		1,10/-1		2,50/-1		1,50/-1		1,50/-1		--	
70	2,90/-1		5,40/-2		5,25/-2		5,25/-2		1,32/-1		7,80/-2		8,30/-2	3		
80	--		--		4,0/ -2		4,0/ -2		--		--		--		--	
90	--		--		--		--		--		--		--		1,35/-1	
100	1,60/-1		--		2,40/-2		--		--		3,75/-2	5	4,25/-2	5	--	
110	1,39/-1		2,0/ -2	1	2,0/ -2		2,0/ -2		4,50/-2		3,40/-2	10	3,70/-2	5	--	
120	1,20/-1		1,85/-2	2	1,80/-2		1,80/-2		3,70/-2		3,30/-2	15	3,40/-2	20	9,0/ -2	
130	--		--		1,10/-2	4	1,10/-2		--		--		--		--	
140	--		--		--		--		--		--		3,0/ -3	20	--	
150	--		1,05/-3	15	--		7,0/ -4		1,50/-2	2	--		1,0/ -3	30	--	
160	4,0/ -2		4,50/-4	20	3,20/-4	5	3,20/-4		--		5,40/-4	20	--		9,50/-3	3
170	--		--		1,60/-4	10	1,60/-4		5,50/-3	2	--		2,50/-4	30	--	
180	2,50/-2		1,90/-4	30	1,0/-4	15	1,0/-4		--		--		--		--	

Table VIII (follows)

Z(cm)	F(Z) Dy(n,γ)	ε%	F(Z) I(n,n')	ε%	F(Z) P(n,p)	ε%	F(Z) S(n,p)	ε%	F(Z) Au/cd	ε%	F(Z) Al(n,p)	ε%	F(Z) Al(n,α)	ε%	F(Z) dose γ	ε%
190	1,95/-2		--		7,0/-5	15	7,0/-5		2,90/-3	2	--		--		--	
200	--		--		5,50/-5	15	5,50/-5		--		1,20/-4	50	1,0/-4	50	--	
210	1,21/-2		1,10/-4	30	4,60/-5	15	4,60/-5		1,70/-3	2	--		--		2,70/-3	5
230	8,50/-3		2,80/-5	50	--		4,10/-5		1,0/-3	2	--		--		--	
232	--		--		--		3,90/-5		9,50/-4	3	--		--		--	
250	4,30/-3		--		--		--		--		--		--		--	
260	--		--		--		--		2,30/-4	3	--		--		--	
270	2,30/-3	1	--		--		--		--		--		--		--	
280	--		--		--		--		1,15/-4	4	--		--		6,95/-4	5
300	1,0/-3	2	--		--		--		--		--		--		--	
320	--		--		--		--		5,0/-5	4	--		--		3,70/-4	10

TABLE IX - (14,2; 98,5; 97,5; 95,5; 27; 15°)

Z(cm)	F(Z) / Dy(n,γ)	ε%	F(Z) / Au/cd	ε %	F(Z) / S(n,p)	ε %	F(Z) / Dose γ	ε %
0	1		1		1		1	
10	9,0/-1		--		--		--	
20	5,90/-1		3,50/-1		2,36/-1		--	
30	3,50/-1		--		--		--	
40	2,20/-1		--		--		2,39/-1	
50	2,37/-1		--		--		--	
60	9,20/-2		3,60/-2		2,40/-2		--	
70	5,90/-2		--		--		--	
80	3,95/-2		1,63/-2		--		--	
90	2,70/-2		--		--		7,0/-2	
100	1,85/-2		8,50/-3		8,0/-3		--	
110	1,30/-2		6,30/-3		6,80/-3		--	
120	9,0/-3		4,45/-3		4,90/-3	2	--	
130	6,20/-3		--		3,10/-3	3	--	
140	4,15/-3		1,90/-3		1,50/-3	5	--	
150	2,70/-3		--		6,50/-4	5	7,0/-3	
160	1,82/-3		7,0/-4		3,30/-4	5	--	
170	1,27/-3		--		--		--	
180	8,80/-4		3,26/-4	2	1,26/-4	8	--	
190	6,10/-4		2,30/-4	3	9,50/-5	8	2,82/-3	
200	4,40/-4		1,68/-4	3	8,40/-5	10	--	
210	3,15/-4	2	1,23/-4	3	7,60/-5	10	--	
220	2,30/-4	2	1,0/-4	5	7,50/-5	8	--	
223,5	2,0/-4	2	9,46/-5	5	7,20/-5	8	--	
230	1,59/-4	3	8,0/-5	5	--		--	

Table IX (follows)

Z(cm)	F(Z) Dy(n,γ)	ε%	F(Z) Au/cd	ε%	F(Z) S(n,p)	ε%	F(Z) Dose γ	ε%
240	1,10/-4	3	5,30/-5	5	6,70/-5	10	---	
250	7,0/-5	3	2,65/-5	5	--		1,20/-3	2
260	4,9/-5	5	1,50/-5	5	---		---	
270	3,55/-5	5	---		---		---	
280	2,90/-5	5	7,10/-6		--		--	
290	2,50/-5	5	5,85/-6	6	3,39/-6	30	5,90/-4	5

TABLE X - (14,2; 96,5; 140,5; 93,5; 10; 45°)

Z(cm)	F(Z) Dy(n,γ)	ε%	F(Z) Au/cd	ε %	F(Z) S(n,p)	ε%	F(Z) doseγ	ε %
0	1		1		1		1	
10	9,50/-1		--		--		--	
20	--		3,40/-1		2,30/-1		--	
30	4,0/-1		--		--		--	
40	--		1,05/-1		5,70/-2		2,45/-1	
60	9,50/-2		3,60/-2		2,22/-2		--	
70	6,40/-2		--		--		--	
80	4,30/-2		1,50/-2		1,15/-2		--	
90	3,0/-2		--		--		7,0/-2	
100	--		8,0/-3		7,40/-3		6,0/-2	
110	1,35/-2		--		--		--	
120	7,50/-3		1,70/-3	1	2,20/-4	2	1,28/-2	
130	4,40/-3		--		--		--	
140	2,60/-3		3,0/-4	2	2,85/-5	8	--	
150	1,60/-3		1,80/-4	2	--		4,30/-3	
160	1,0/-3		--		--		--	
170	6,50/-4	1	8,50/-5	3	9,0/-6	8	--	
180	4,46/-4	2	6,30/-5	6	6,60/-6	8	--	
190	2,90/-4	2	--		--		1,10/-3	
200	2,10/-4	2	3,45/-5	6	4,10/-6	10	--	
210	1,50/-4	4	--		--		--	
220	1,18/-4	4	--		--		4,0/-4	2
230	9,50/-5	4	--		--		2,80/-4	2
240	8,10/-5	4	1,20/-5	8	2,19/-6	20	--	
250	3,70/-5	5	--		--		--	

Table X (follows)

Z(cm)	F(Z) Dy(n,γ)	ε %	F(Z) Au/cd	ε %	F(Z) S(n,p)	ε%	F(Z) dose γ	ε%
260	—		2,90/-6	10	—		1,27/-4	5
270	1,20/-5	8	—		—		9,80/-5	8
280	7,60/-6	10	1,40/-6	30	—		—	
290	—		—		—		6,0/-5	8
300	3,40/-6	20	—		—		4,90/-5	8
310	2,30/-6	15	—		—		4,0/-5	10
320	1,68/-6	20	7,50/-7	50	5,60/-7	30	—	
330	1,20/-6	30	—		—		2,80/-5	10

TABLE XI - (28,7; 107,7; 145,7; 110; 16,5; 60°)

Z(cm)	F(Z) Dy(n,γ)	ε %	F(Z) In(n,n')	ε%	F(Z) Au/cd	ε %	F(Z) S(n,p)	ε%	F(Z) Al(n,α)	ε %	F(Z) Dose γ	ε %
0	1		1		1		1		1		1	
10	1		--		--		--		--		--	
20	--		--		5,90/-1		4,30/-1		--		--	
30	6,90/-1		--		--		--		--		4,90/-1	
40	--		--		--		--		--		3,95/-1	
50	--		1,10/-1		2,20/-1		1,10/-1		1,50/-1		--	
60	3,60/-1		--		--		--		1,05/-1		--	
70	--		--		--		--		7,60/-2		--	
80	2,30/-1		--		8,95/-2		4,40/-2		--		1,76/-1	
90	--		--		--		--		4,49/-2		--	
100	1,50/-1		2,73/-2		5,20/-2		2,73/-2		--		1,22/-1	
110	1,22/-1		2,35/-2		4,20/-2		2,35/-2		3,20/-2	2	1,05/-1	
120	1,03/-1		1,99/-2		3,50/-2		1,99/-2		2,70/-2	3	9,10/-2	
123,5	9,50/-2		1,22/-2		3,20/-2		1,22/-2		2,43/-2	5	8,0/-2	
130	8,30/-2		3,40/-3		2,10/-2		3,40/-3	3	4,23/-3	10	--	
140	6,15/-2		--		1,30/-2		8,50/-4	3	6,40/-4	30	2,10/-2	
150	4,66/-2		--		--		3,40/-4	5	1,80/-4	40	--	
170	2,58/-2		--		--		--		--		7,50/-3	
180	--		--		2,90/-3		7,50/-5	10	--		5,65/-3	
190	1,55/-2		7,10/-5	25	2,18/-3	1	5,49/-5	10	--		--	

Table XI (follows)

Z(cm)	F(Z) Dy(n,γ)	ε%	F(Z) In(n,n')	ε%	F(Z) Au/cd	ε%	F(Z) S(n,p)	ε%	F(Z) Al(n,α)	ε%	F(Z) dose γ	ε%
200	1,20/-2		--		--		--		--		3,20/-3	
210	9,50/-3		--		1,20/-3	2	3,0/-5	10	--		--	
220	7,80/-3		--		9,50/-4	2	2,35/-5	10	--		1,88/-3	
230	--		2,85/-5	30	--		--		--		1,43/-3	
240	5,0/-3		--		--		--		--		--	
250	4,30/-3		--		4,75/-4	4	1,25/-5	15	--		8,90/-4	
260	3,50/-3		1,75/-5	40	--		--		--		--	
270	2,70/-3		1,40/-5	40	3,20/-4	4	1,19/-5	15	--		5,45/-4	1
280	1,98/-3		1,10/-5	50	--		--		--		--	
290	1,40/-3		--		7,30/-5	6	5,0/-6	20	--		--	
300	1,03/-3		--		--		2,90/-6	35	--		2,10/-4	3
310	8,0/-4	1	--		3,10/-5	10	1,90/-6	35	--		1,60/-4	3
320	6,45/-4	1	--		--		--		--		--	
330	5,20/-4	1	--		1,55/-5	15	--		--		1,10/-4	4
340	4,48/-4	1	--		1,19/-5	15	--		--		--	
350	3,80/-4	2	--		--		--		--		--	
360	3,40/-4	2	--		8,30/-6	15	--		--		8,49/-5	5

TABLE XII - (28,7; 166; 127; 122; 14,3; 90°)

Z(cm)	F(Z) Dy(n,γ)	ε %	F(Z) In(n,γ)	ε %	F(Z) In(n,n')	ε %	F(Z) P(n,p)	ε %	F(Z) dose γ	ε %
0	1		1		1		1		1	
10	1		--		--		--		--	
20	8,9/-1		6,13/-1		--		--		--	
30	7,4/-1		--		--		2,50/-1		--	
40	6,0/-1		--		1,62/-1	2	--		3,7/-1	
50	4,80/-1		2,14/-1		--		--		--	
60	3,60/-1		--		--		7,50/-2		--	
70	--		--		--		--		--	
80	2,25/-1		9,30/-2		3,80/-2	3	--		--	
90	--		--		--		--		1,50/-1	
100	1,50/-1		5,45/-2		--		--		--	
110	1,20/-1		--		--		--		--	
120	1,0/-1		3,42/-2		1,80/-2	3	1,80/-2		9,50/-2	
130	8,50/-2		--		--		--		--	
140	6,95/-2		2,40/-1		--		--		7,70/-2	
150	5,80/-2		--		--		--		6,95/-2	
160	4,95/-2		1,71/-2		1,10/-2	4	1,14/-2	5	6,20/-2	
170	4,60/-2		--		--		--		5,90/-2	
180	3,90/-2		--		6,80/-3	5	4,40/-3	10	3,79/-2	

Table XII (follows)

Z(cm)	F(Z) Dy(n, γ)	ε%	F(Z) In(n,γ)	ε%	F(Z) In(n,n')	ε%	F(Z) P(n,p)	ε%	F(Z) dose γ	ε%
190	2,60/-2		4,18/-3		2,50/-4	10	3,30/-4	20	--	
200	1,85/-2		--		8,5/-5	30	1,10/-4	20	5,90/-3	
210	1,35/-2		1,71/-3		--		5,50/-5	20	4,10/-3	2
220	1,03/-2		--		--		--		--	
230	8,0/-3		--		--		2,08/-5	100	--	
240	6,20/-3		6,43/-4		--		1,40/-5	100	1,65/-3	3
250	4,96/-3		4,82/-4		--		1,0/-5	100	--	
260	3,90/-3		--		--		--		--	
270	3,06/-3		--		--		--		6,70/-4	3
280	2,50/-3	1	2,14/-4		--		--		--	
290	1,95/-3	1	--		--		--		3,60/-4	4
300	--		--		--		--		--	
310	1,30/-3	1	5,50/-5	2	--		--		2,59/-4	4
320	9,0/-4	1	2,90/-5	3	--		--		--	
330	6,20/-4	1	--		--		--		--	
340	4,50/-4	1	--		--		--		--	
350	3,40/-4	1	8,95/-6	4	--		--		1,15/-4	4
360	2,63/-4	1	--		--		--		--	
370	2,10/-4	1	--		--		--		--	
380	1,68/-4	1,5	--		--		--		5,70/-5	5

Table XII (follows)

Z(cm)	F(Z) Dy(n,γ)	ε%	F(Z) In(n,γ)	ε%	F(Z) In(n,n')	ε%	F(Z) P(n,p)	ε%	F(Z) dose γ	ε %
390	1,40/-4	1,5	3,85/-6	6	--		--		--	
400	1,20/-4	1,5	--		--		--		--	
410	1,10/-4	1,5	--		--		--		3,65/-5	5
420	1,0/-4	1,5	2,45/-6	5	--		--		3,4/-5	5

TABLE XIII - (14,2; 102,3; 145; 116,3; 8,2; 60°)

Z(cm)	F(Z) Dy(n,γ)	ε%	F(Z) In(n,γ)	ε%	F(Z) Au/cd	ε %	F(Z) S(n,p)	ε%	F(Z dose	ε%
0	1		1		1		1		1	
20	6,0/-1		3,20/-1		--		--		--	
30	--		--		--		1,20/-1		--	
40	2,50/-1		--		1,0/-1		--		2,50/-1	
50	--		--		--		4,50/-2		--	
60	1,0/-1		4,0/-2		--		--		--	
70	--		--		2,55/-2		--		1,10/-1	
80	4,30/-2		--		--		--		--	
90	3,0/-2		1,25/-2		1,25/-2		1,03/-2	1	6,50/-2	
100	2,20/-2		--		--		--		5,10/-2	
110	1,65/-2		6,30/-3		6,30/-3		5,0/-3	4	4,0/-2	
120	9,0/-3		2,20/-3		2,20/-3		2,20/-4	5	1,15/-2	
130	5,0/-3		--		1,0/-3		6,50/-5	15	8,20/-3	
140	2,9/-3		--		--		--		6,48/-3	
150	1,78/-3		2,60/-4		2,60/-4		2,5/-5	30	4,98/-3	
160	1,10/-3		1,50/-4	4	1,50/-4	4	--		3,40/-3	
170	7,0/-4		--		9,0/-5	6	--		--	
180	4,48/-4		--		--		--		1,75/-3	
190	2,85/-4		4,20/-5	5	4,20/-5	10	--		1,20/-3	

Table XIII (follows)

Z(cm)	F(Z) Dy(n,γ)	ε %	F(Z) In(n,γ)	ε %	F(Z) Au/cd	ε %	F(Z) S(n,p)	ε %	F(Z) dose γ	ε %
200	2,0/-4		--		3,0 /-5	15	--		--	
210	1,40/-4		--		--		--		5,40/-4	
220	1,0 /-4		1,70/-5	5	1,70/-5	20	--		3,0 /-4	
230	7,60/-5	1	--		--		--		--	
240	6,0 /-5	2	1,06/-5	10	1,06/-5	25	--		1,40/-4	
250	--		--		9,0 /-6	20	--		1,10/-4	2
260	3,50/-5	3	3,60/-6	20	3,60/-6	20	--		8,90/-5	3
270	1,80/-5	3	1,60/-6	20	--		--		--	
280	9,5 /-6	5	--		--		--		6,40/-5	4
290	5,5 /-6	10	6,20/-7	20	--		--		--	
300	3,40/-6	20	4,45/-7	20	--		--		4,40/-5	4
310	2,20/-6	20	--		--		--		3,50/-5	5
320	1,53/-6	20	2,63/-7	20	--		--		--	
330	--		--		--		--		--	
340	8,15/-7	40	--		--		--		1,70/-5	5
350	6,48/-7	50	--		--		--		1,35/-5	10
360	5,0 /-7	60	1,40/-7	100	--		--		1,07/-5	10
370	4,0 /-7	60	--		--		--		--	

TABLE XIV - (14,2; 142,4; 125; 147; 7,1; 90°)

Z(cm)	F(Z) / Dy(n,γ)	ε %	F(Z) / dose γ	ε %
0	1		1	
20	6,30/-1		--	
40	2,50/-1		--	
70	6,20/-2		1,02/-1	
90	2,77/-2		--	
110	1,4 /-2		4,20/-2	
140	6,50/-3		2,40/-2	
150	4,30/-3		1,30/-2	
160	2,20/-3		4,0 /-3	
170	1,27/-3		--	
180	7,50/-4		--	
190	4,50/-4		2,30/-3	3
200	2,87/-4	3	--	
210	1,83/-4	3	--	
220	1,20/-4	4	--	
230	7,60/-5	5	--	
240	5,0 /-5	6	4,80/-4	4
250	3,67/-5	8	2,90/-4	5
260	3,0 /-5	8	1,70/-4	5
270	2,70/-5	5	--	
280	1,30/-5	15	--	
290	6,70/-6	15	--	
310	2,10/-6	15	--	
330	9,50/-7	20	--	
390	1,45/-7	50	--	
410	7,60/-8	100	--	

TABLE XV - (28,7; 166 + 74; 127; 122; 14,3; 90°)

Z(cm)	F(Z) / Dy(n,γ)	ε %	F(Z) / P(n,p)	ε %
29	--		2,87/-1	
30,2	7,17/-1		--	
50,5	4,75/-1		--	
59,5	--		7,50/-2	1
81	2,35/-1		--	
101,8	1,46/-1		--	
108	1,26/-1		--	
125	--		1,75/-2	2
132	7,82/-2		--	
149	5,35/-2		--	
164	3,63/-2		--	
165	--		1,00/-2	2
176	2,62/-2		--	
184	--		1,03/-3	4
199	2,12/-2		--	
194	--		1,36/-4	5
204	--		5,40/-5	10
215	--		2,80/-5	20
226	--		2,20/-5	20
240	1,56/-2		--	
247	--		6,40/-6	40
181	2,39/-2		--	

Table XV (follows)

Z(cm)	F (Z) / Dy(n, γ)	ε %	F(Z) / P(n,p)	ε %
191	1,60/-2		--	
202	1,16/-2		--	
212	8,42/-3		--	
223	6,27/-3		--	
234	4,76/-3		--	
244	3,79/-3		--	
255	2,97/-3		--	
266	2,22/-3		--	
276	1,83/-3	1	--	
291	1,36/-3	1	--	
306	1,05/-3	2	--	
323	5,25/-4	2	--	
335	3,58/-4	2	--	
349	2,56/-4	2	--	
356	2,02/-4	2	--	
364	1,66/-4	2	--	
372	1,36/-4	2	--	
381	1,16/-4	2	--	
389	9,75/-5	2	--	
397	8,55/-5	2	--	
406	7,96/-5	2	--	
415	7,21/-5	2	--	

TABLE XVI - (28,7; 108 + 92; 104; 111; 20; 45°)

Z (cm)	F(Z) Dy(n, γ)	ε%	F(Z) In(n,γ)	ε%	F(Z) Au/cd	ε%	F(Z) P(n,p)	ε%	F(Z) S(n,p)	ε%
0	1		1		1		1		1	
10,2	1,04		--		--		--		--	
10,4	--		--		8,92/-1		--		--	
10,8	--		--		--		--		7,14/-1	
20,1	--		6,3 /-1	2	--		--		--	
29,3	--		--		--		2,75/-1		--	
30,3	--		4,5 /-1	2	--		--		--	
30,5	--		--		4,6 /-1		--		--	
30,9	--		--		--		--		2,48/-1	
49,5	--		--		--		1,1 /-1		--	
50,5	--		2,42/-1	2	--		--		--	
51,3	--		--		2,34/-1		--		--	
69,6	--		--		--		5,32/-2		--	
70,9	3,08/-1		--		1,32/-1		--		--	
71,3	--		--		--		--		5,2 /-2	
80	--		--		--		4,2/-2	1	--	
81	--		1,05/-1	1	--		--		--	
102	1,36/-1		5,75/-2	1	5,5 /-2		--		--	
112	--		--		--		1,98/-2	1	--	

Table XVI (follows)

Z(cm)	F(Z) Dy(n,γ)	ε %	F(Z) In(n,γ)	ε %	F(Z) Au/cd	ε %	F(Z) P(n,p)	ε%	F(Z) S(n,p)	ε %
113	—		—		4,21/-2		—		2,02/-2	
118	9,22/-2		3,66/-2	1	—		—		—	
122	—		—		2,87/-2		1,88/-2	1	—	
123	—		—		—		—		1,72/-2	1
125	7,59/-2		—		—		—		—	
126	—		2,72/-2	1	—		—		—	
133	6,15/-2		—		1,73/-2		7,1 /-3	2	—	
134	—		—		—		—		4,8 /-3	2
143	—		1,24/-2	1	—		—		—	
150	3,98/-2		—		8,74/-3		—		4,7 /-4	3
157	—		1,88/-2*	1	—		—		—	
158	—		—		—		3,7 /-4	10	—	
159	—		7,1 /-3	2	1,86/-2*		—		—	
160	—		—		—		—		1,17/-2*	1
163	5,19/-2*		—		—		—		—	
165	—		—		—		2,1 /-4	10	—	
167	—		—		5,02/-3		—		1,90/-4	6
175	2,18/-2		—		—		—		—	
176	—		4,3 /-3	2	—		—		—	

Table XVI (follows)

Z(cm)	F(Z) Dy(n,γ)	ε%	F(Z) In(n,γ)	ε%	F(Z) Au/cd	ε%	F(Z) P(n,p)	ε%	F(Z) S(n,p)	ε%
184	--		--		2,92/-3		--		--	
185	--		--		--		--		1,1 /-4	2
192	--		--		2,01/-3	1	--		--	
193	--		--		--		--		7,2 /-5	7
195	--		--		--		9,0 /-5	15	--	
202	--		--		--		6,0 /-5	15	--	
207	1,08/-2		--		--		--		--	
209	--		--		2,06/-3	1	--		4,3 /-5	2
210	--		1,76/-3	2	--		--		--	
220	8,44/-3		--		--		--		--	
223	--		1,22/-3	2	--		--		--	
226	7,45/-3		--		--		--		--	
229	--		1,06/-3	3	--		--		--	
230	--		--		9,14/-4	1	--		4,3 /-5	3
231	6,71/-3		--		--		5,0 /-5	15	--	
243	--		--		3,85/-4	1,5	--		--	
244	--		--		--		--		1,2 /-5	4
252	3,55/-3		--		--		--		--	
259	--		--		2,1 /-4	3	--		2,0 /-6	15

Table XVI (follows)

Z(cm)	F(Z) Dy(n, γ)	ε%	F(Z) In(n, γ)	ε %	F(Z) Au/cd	ε %	F(Z) P(n, p)	ε %	F(Z) S(n, p)	ε %
260	--		2,4 /-4	3	--		--		--	
272	2,08/-3		--		--		--		--	
281	--		1,23/-4	4	--		--		--	
288	--		--		8,4 /-5	4	--		5,0 /-7	50
300	1,08/-3		--		--		--		--	
301	--		7,2 /-5	5	--		--		--	
320	--		--		3,9 /-5	8	--		3,0 /-7	50

* Points on the extension of the first leg.

TABLE XVII

Unreflected thermal neutron current $j^{\circ}(Z)$ entering the cylindrical wall of a straight duct; wall material: aluminum; duct radius: a.

a = 5 cm		a = 15 cm	
Z (cm)	$j^{\circ}(Z)$ ($n/cm^2 s$)	Z (cm)	$j^{\circ}(Z)$ ($n/cm^2 s$)
1,4	2,86/6	5	2,7/6
3	4,3/6	34	5,8/6
5	3,26/6	50	2,4/5
11	1,83/6	95	7,3/4
32	9,7/4	125	3,2/4
62	1,0/4	185	9,1/3
102	1,33/3	270	4,7/3
202	1,40/2		
278	8,1/1		

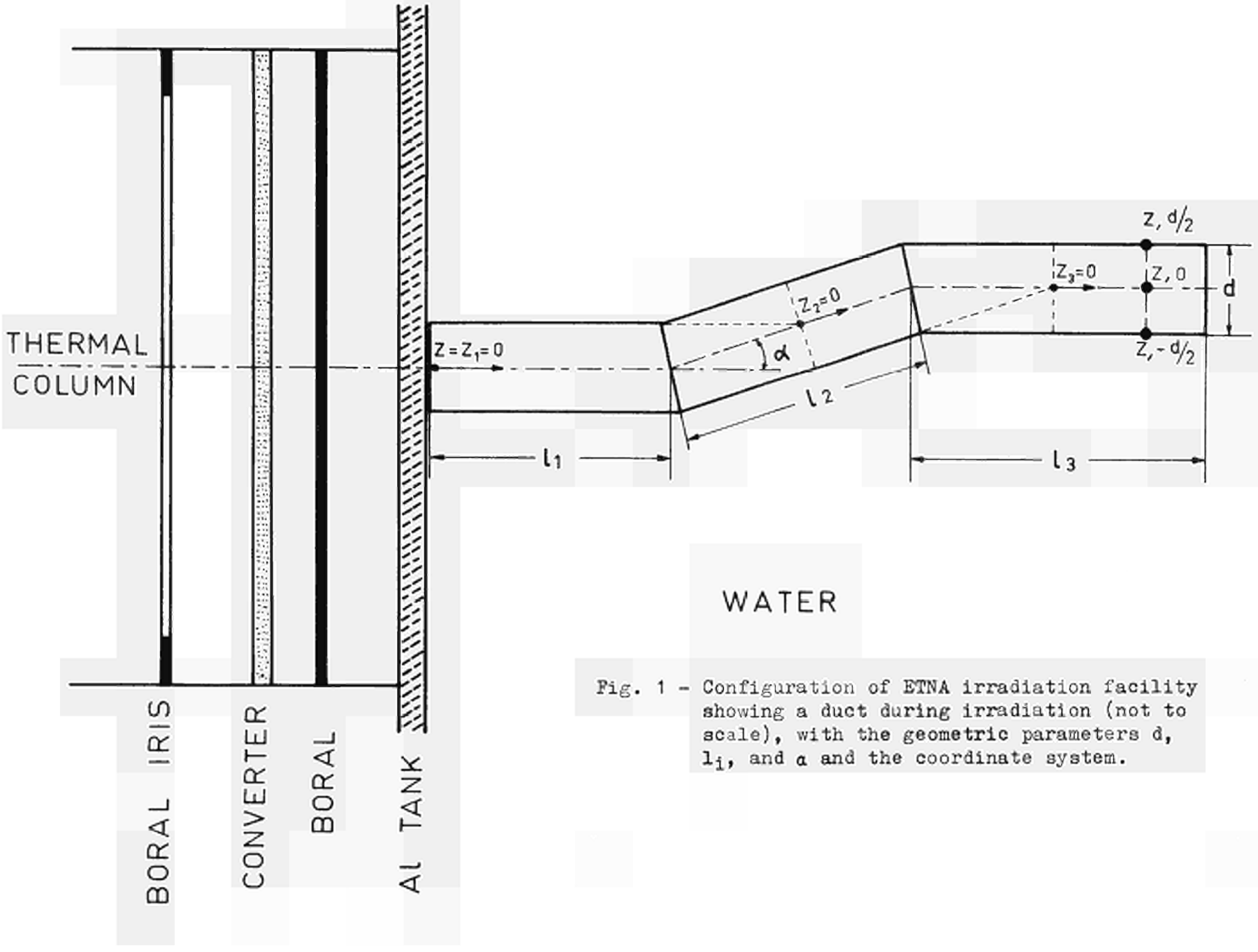

Fig. 1 - Configuration of ETNA irradiation facility showing a duct during irradiation (not to scale), with the geometric parameters d, l_i, and α and the coordinate system.

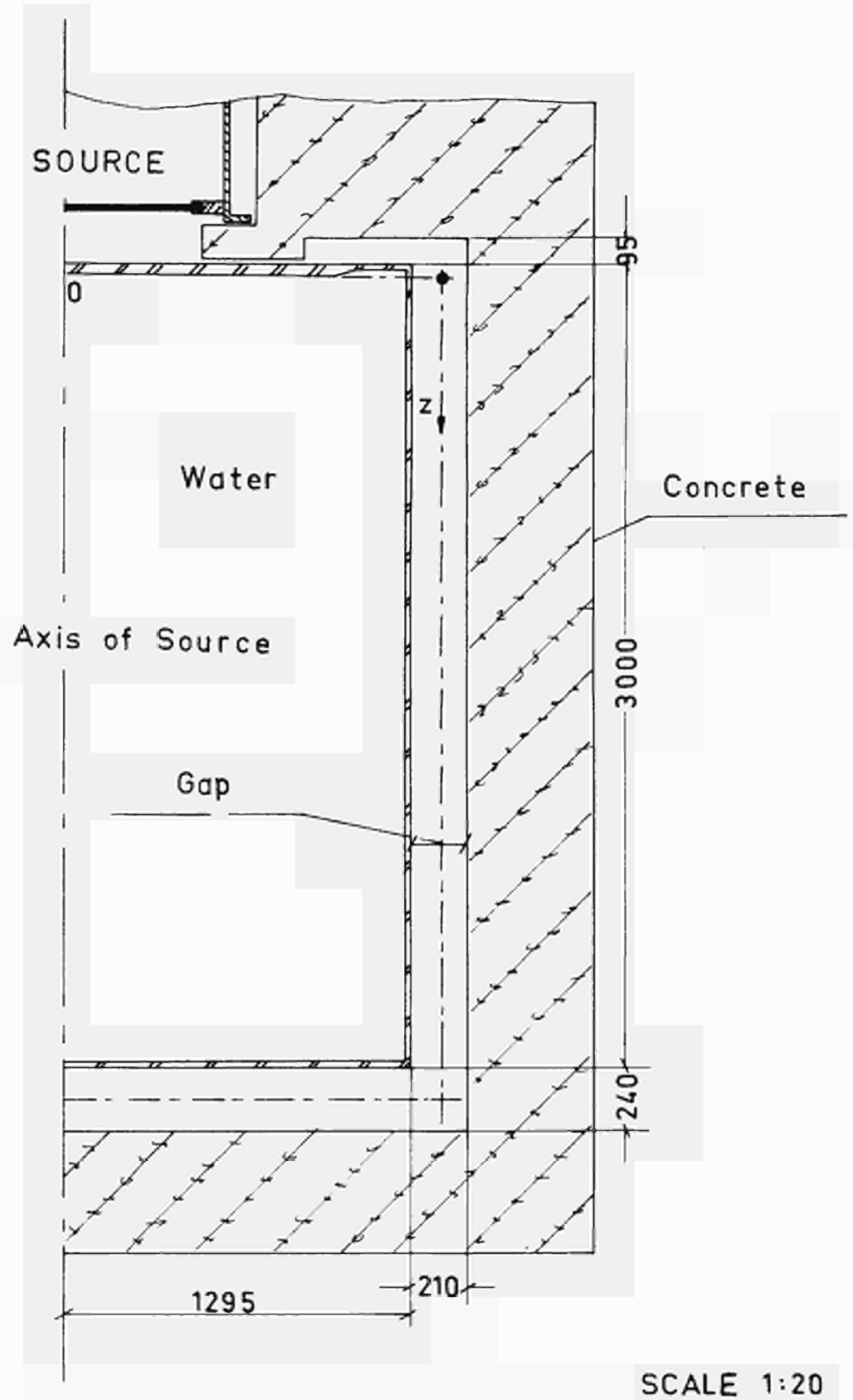

Fig. 2 - Horizontal section of ETNA tank.

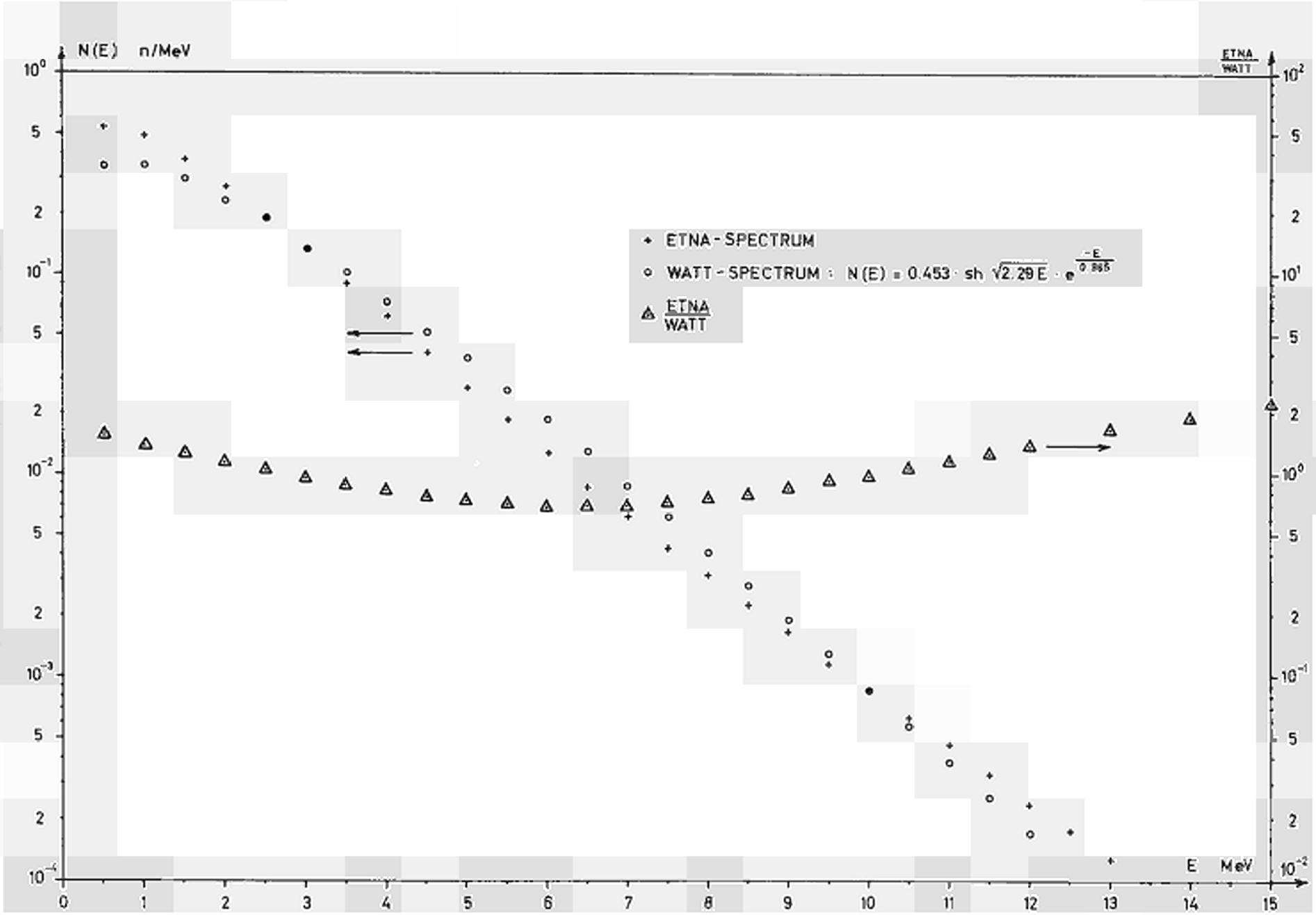

Fig. 3 - Neutron source spectrum.

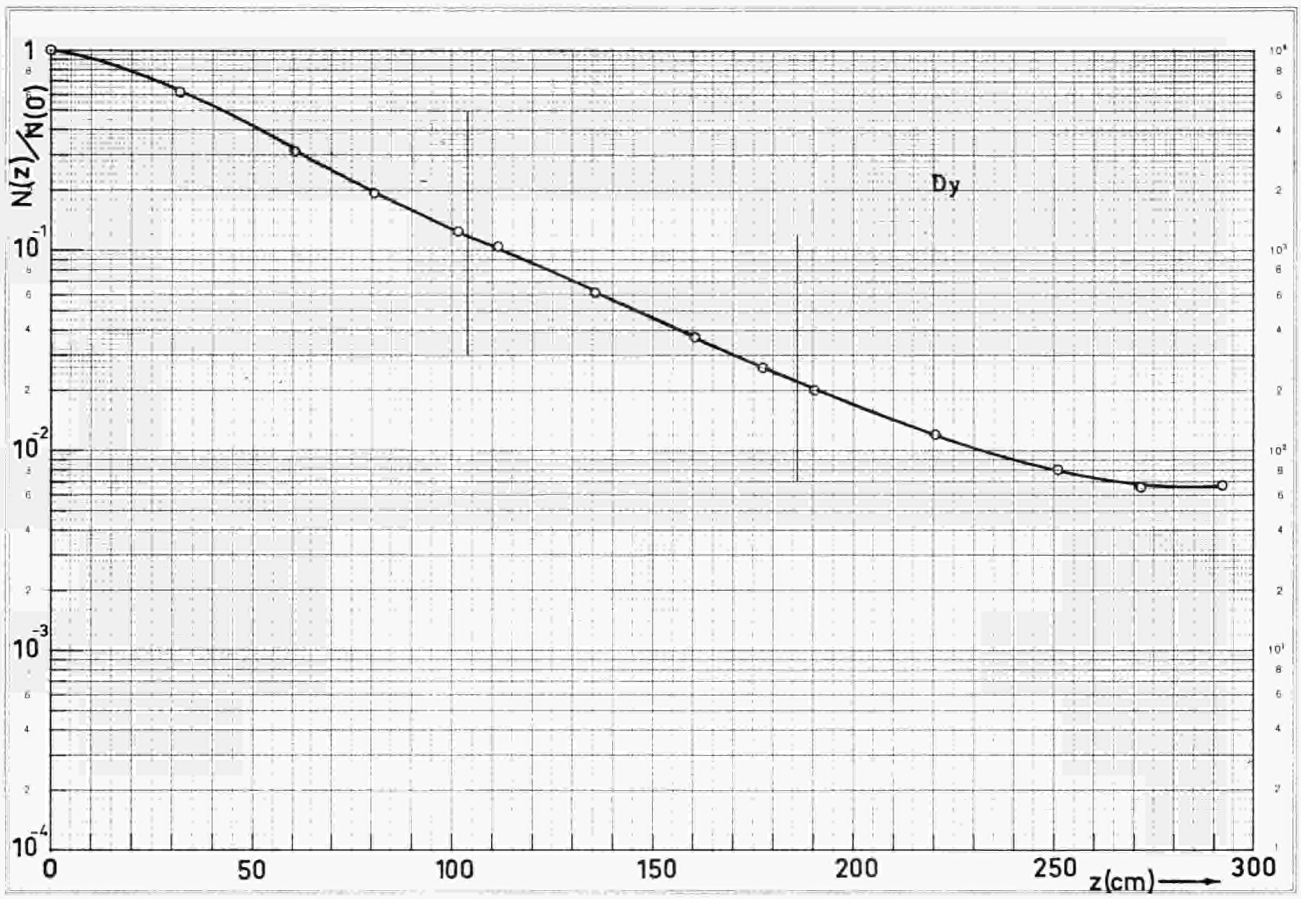

Fig. 4 - Thermal activation rates in configuration 1a.

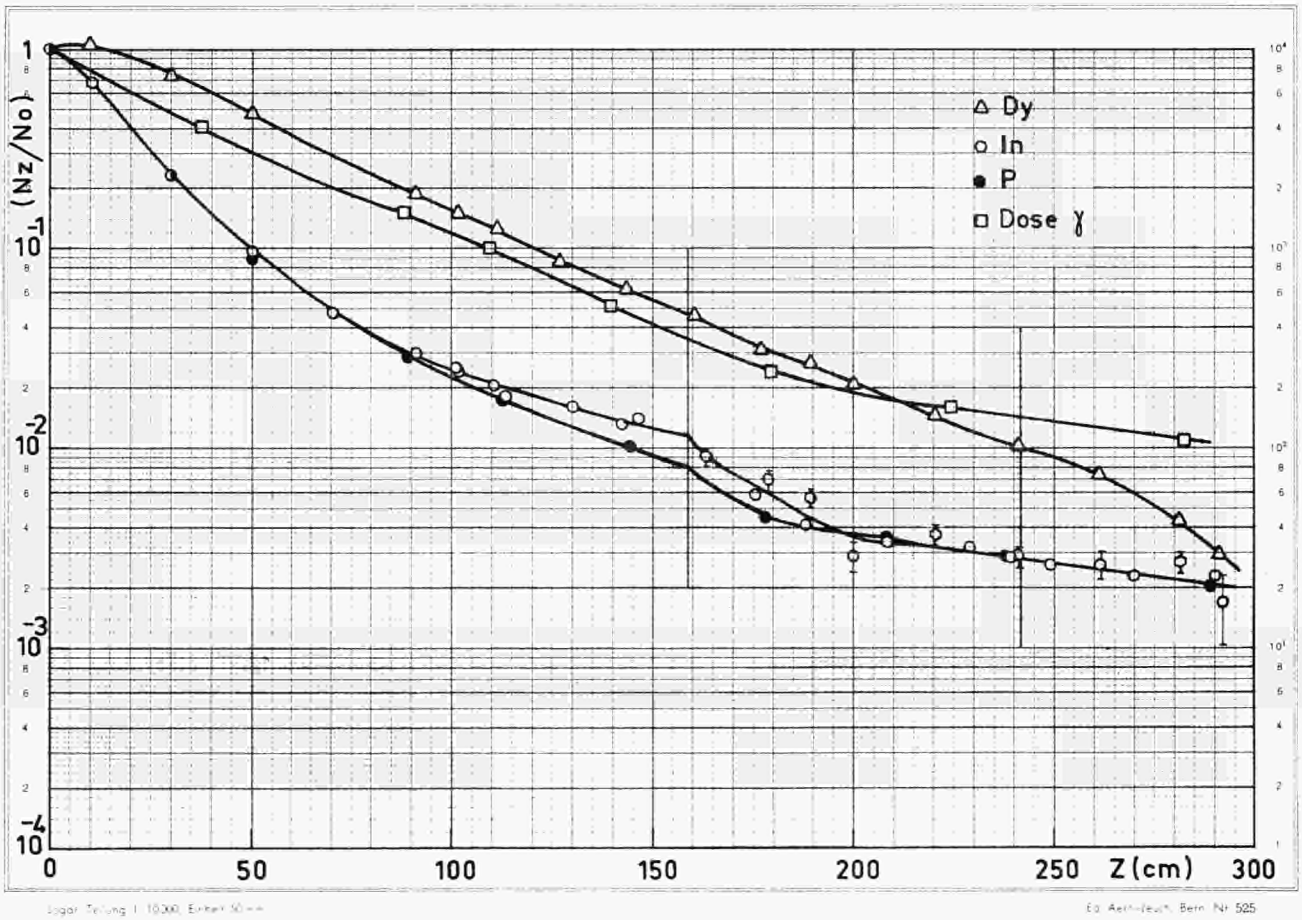

Fig. 5 - Fast, thermal activation rates and γ doses in configuration 1b.

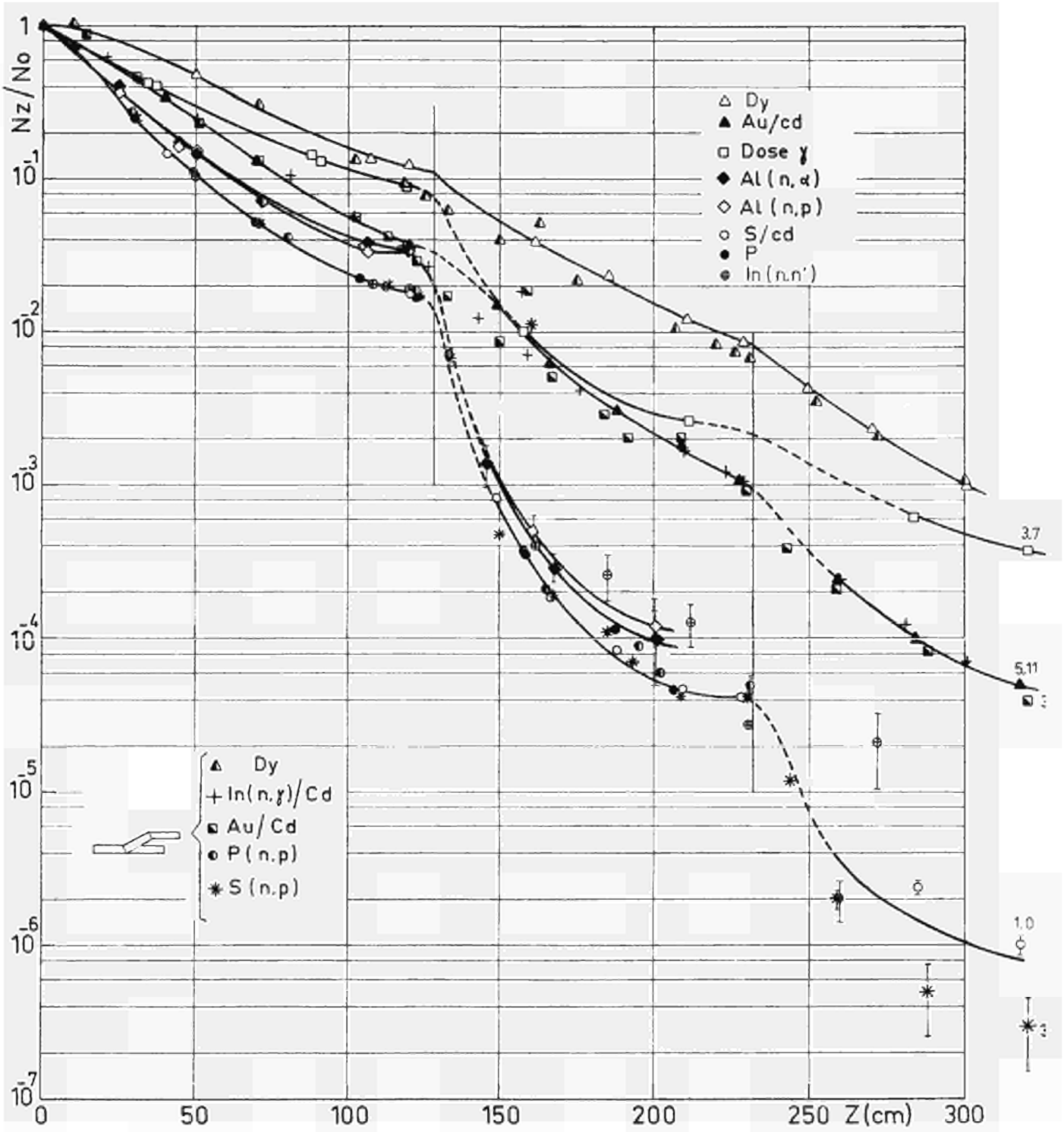

Fig. 6 - Fast, epithermal and thermal activation rates and γ doses in configuration 10 and 2, with and without cavity.

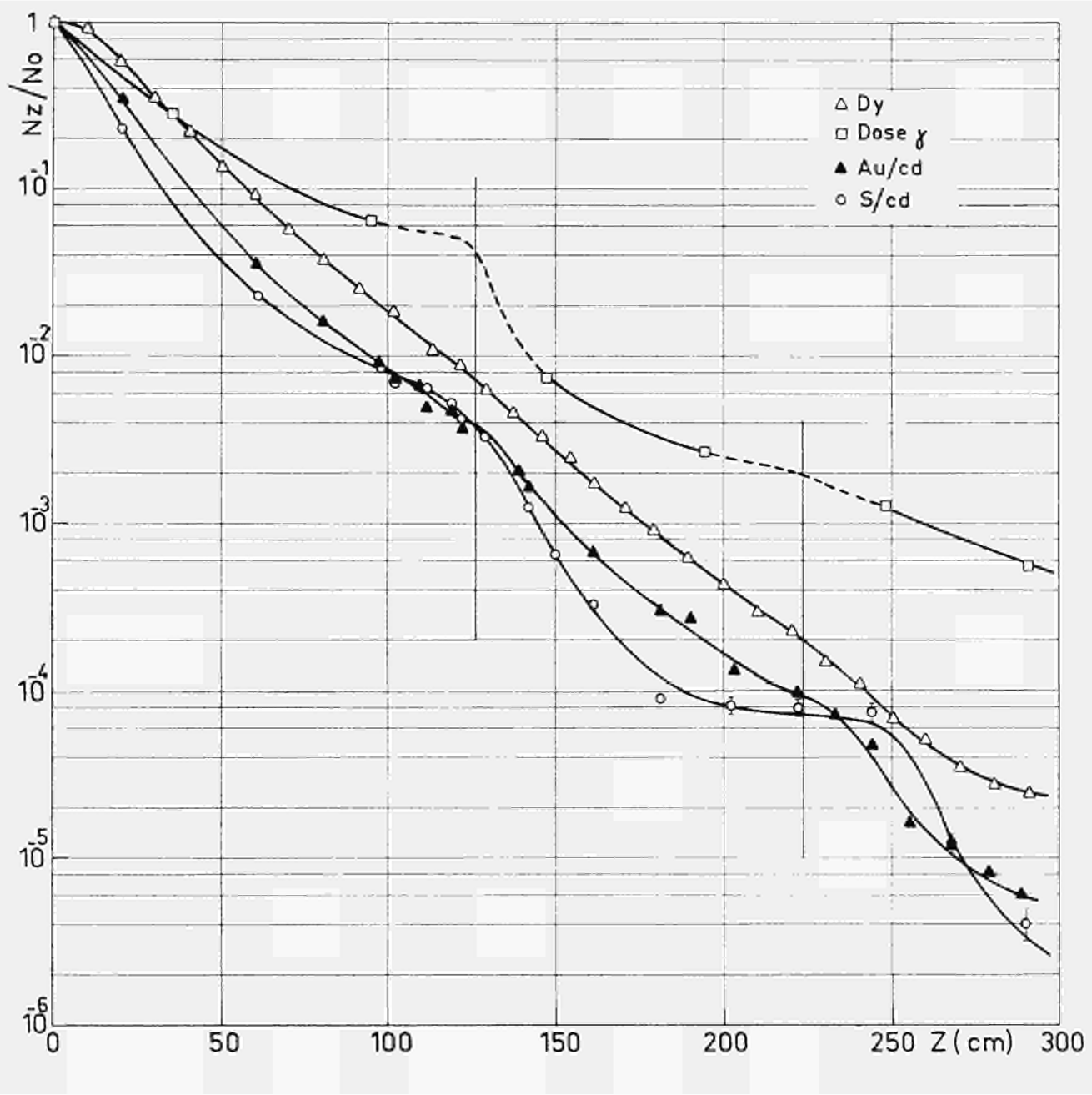

Fig. 7 - Fast, epithermal and thermal activation rates and γ doses in configuration 3.

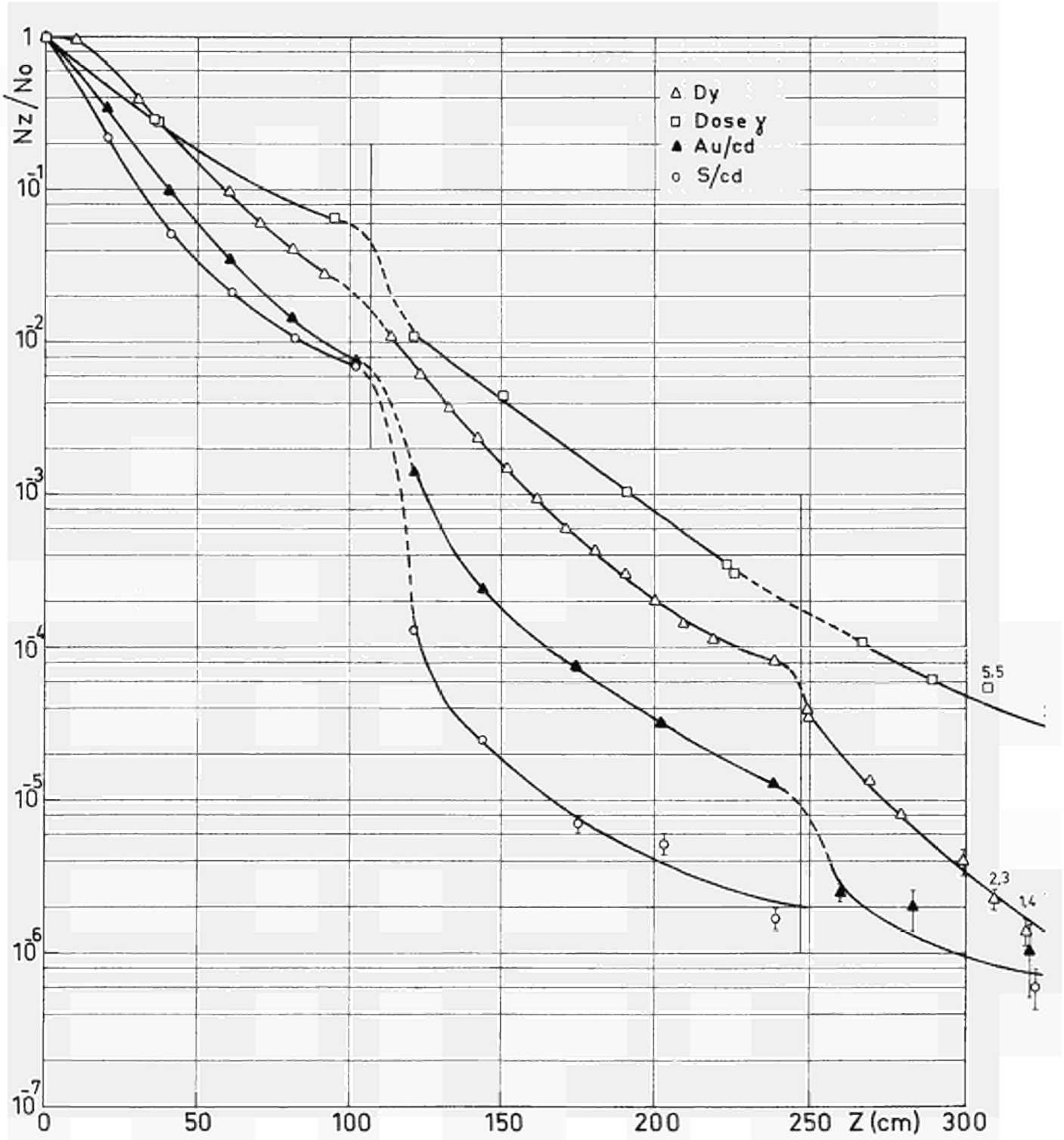

Fig. 8 - Fast, epithermal and thermal activation rates and γ doses in configuration 4.

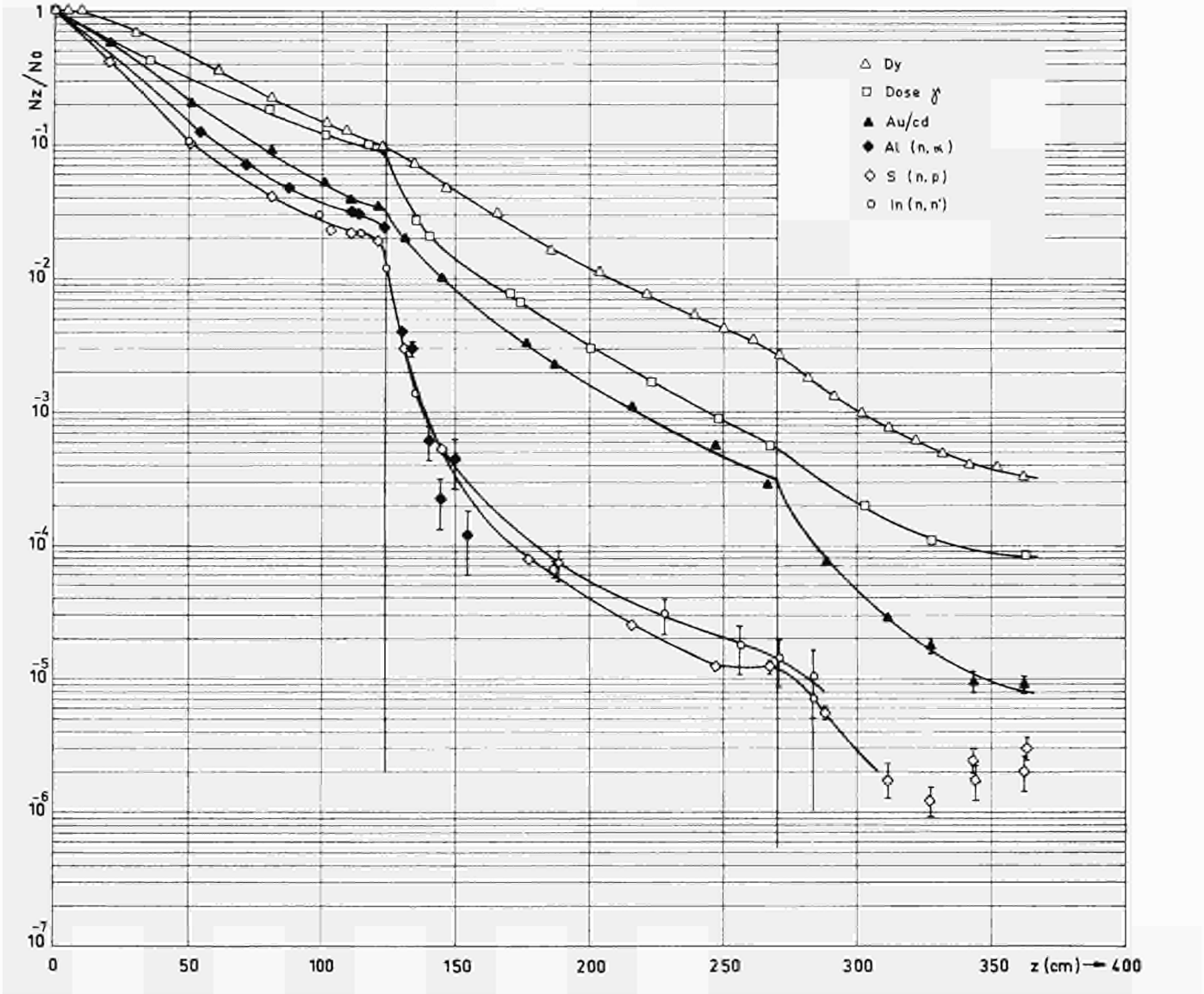

Fig. 9 - Fast, epithermal and thermal activation rates and γ doses in configuration 5.

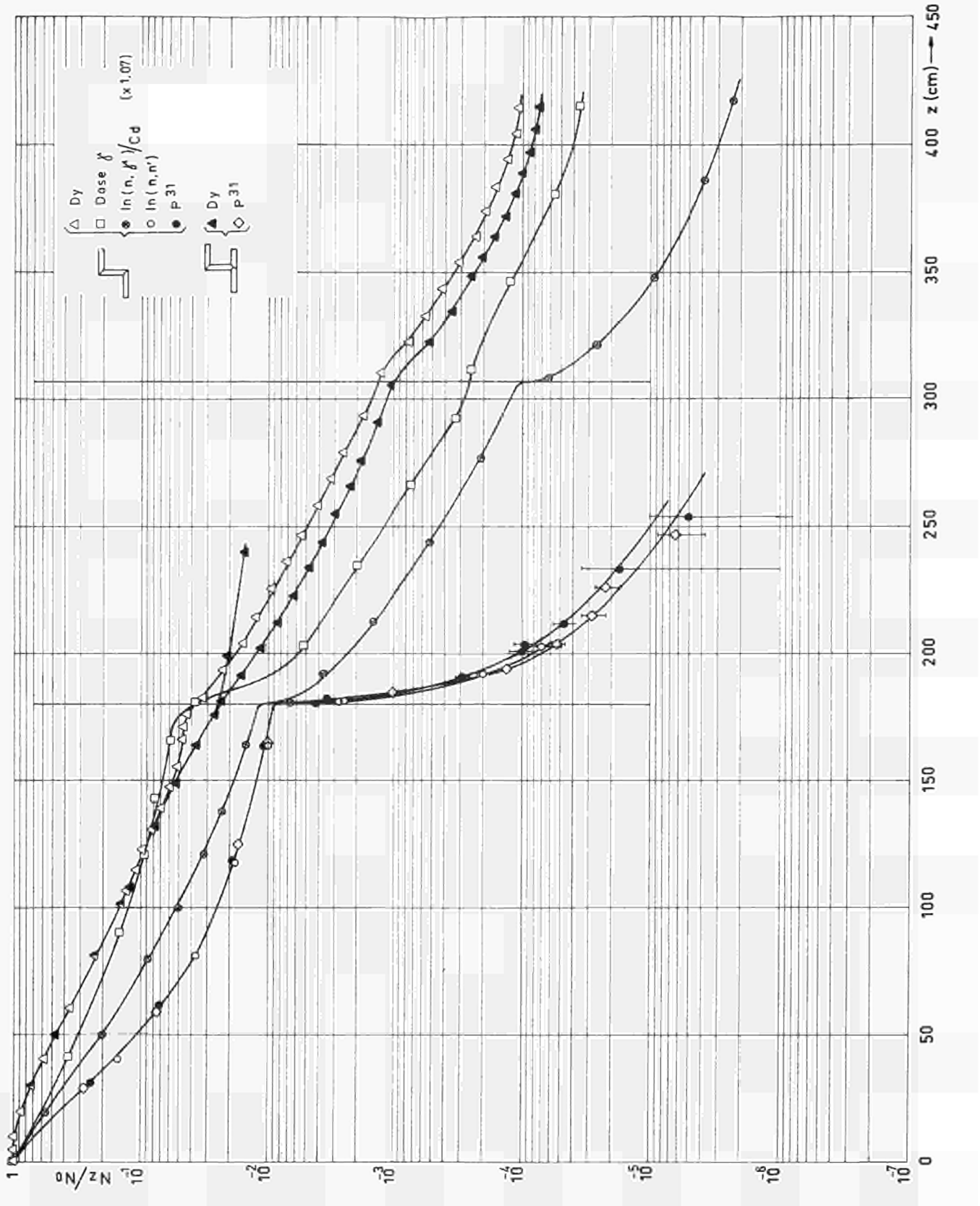

Fig. 10 - Fast, epithermal and thermal activation rates and γ doses in configuration 9 and 6 with and without cavity.

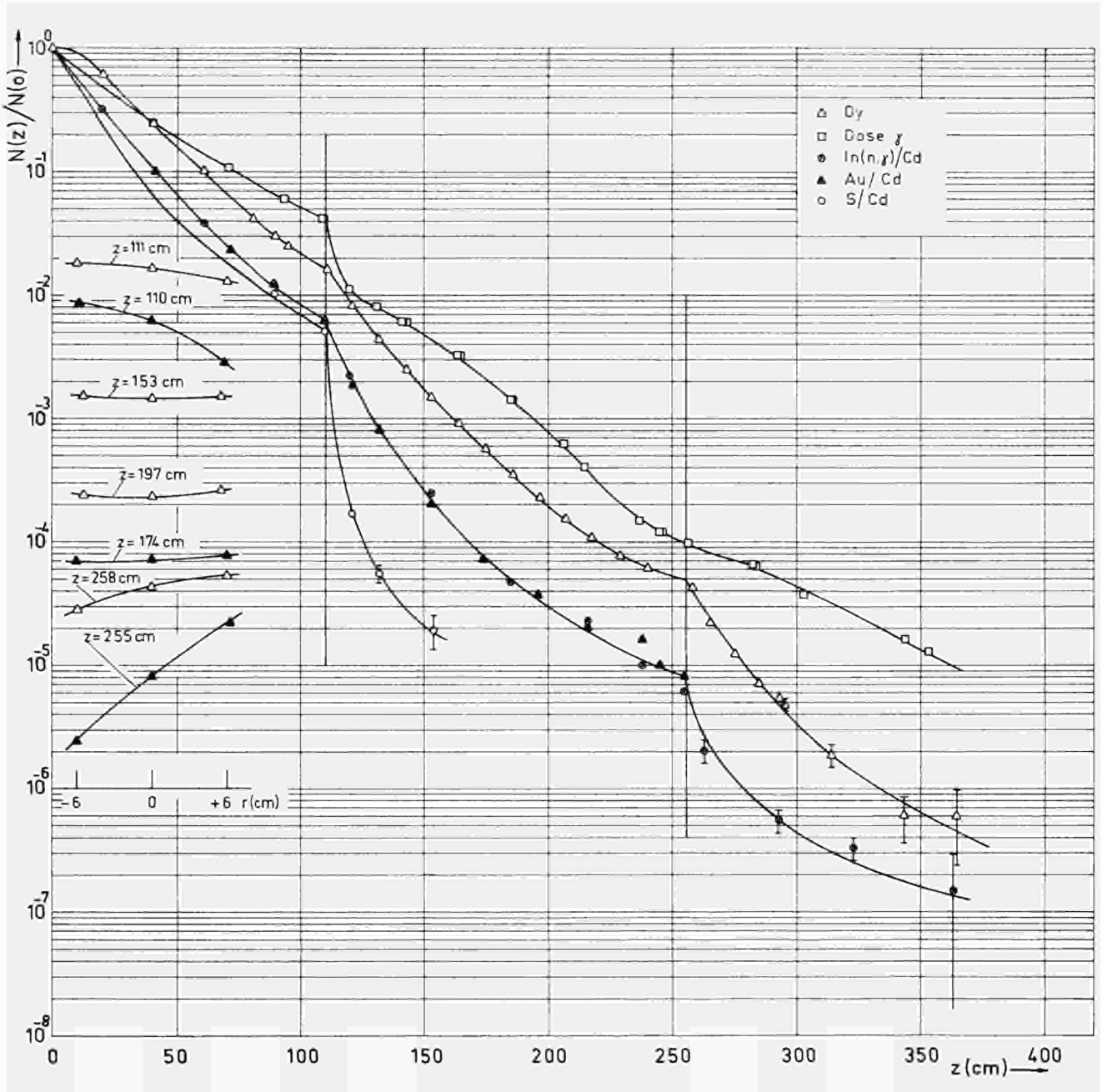

Fig. 11 - Fast, epithermal and thermal activation rates and γ doses in configuration 7.
Some radial distribution at various Z are shown in the insert.

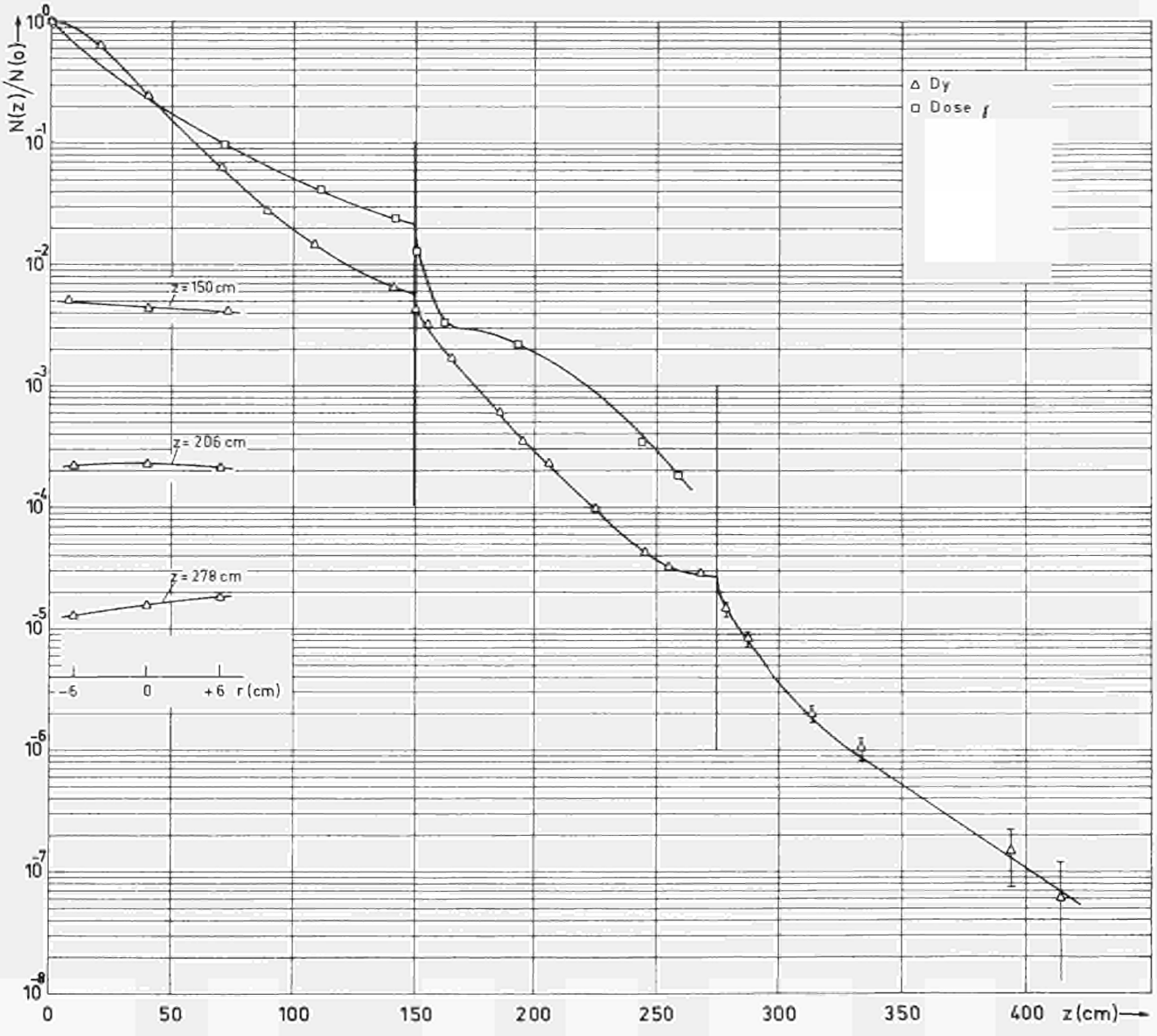

Fig. 12 - Thermal activation rates and γ doses in configuration 8. Some radial distribution at various Z are shown in the insert.

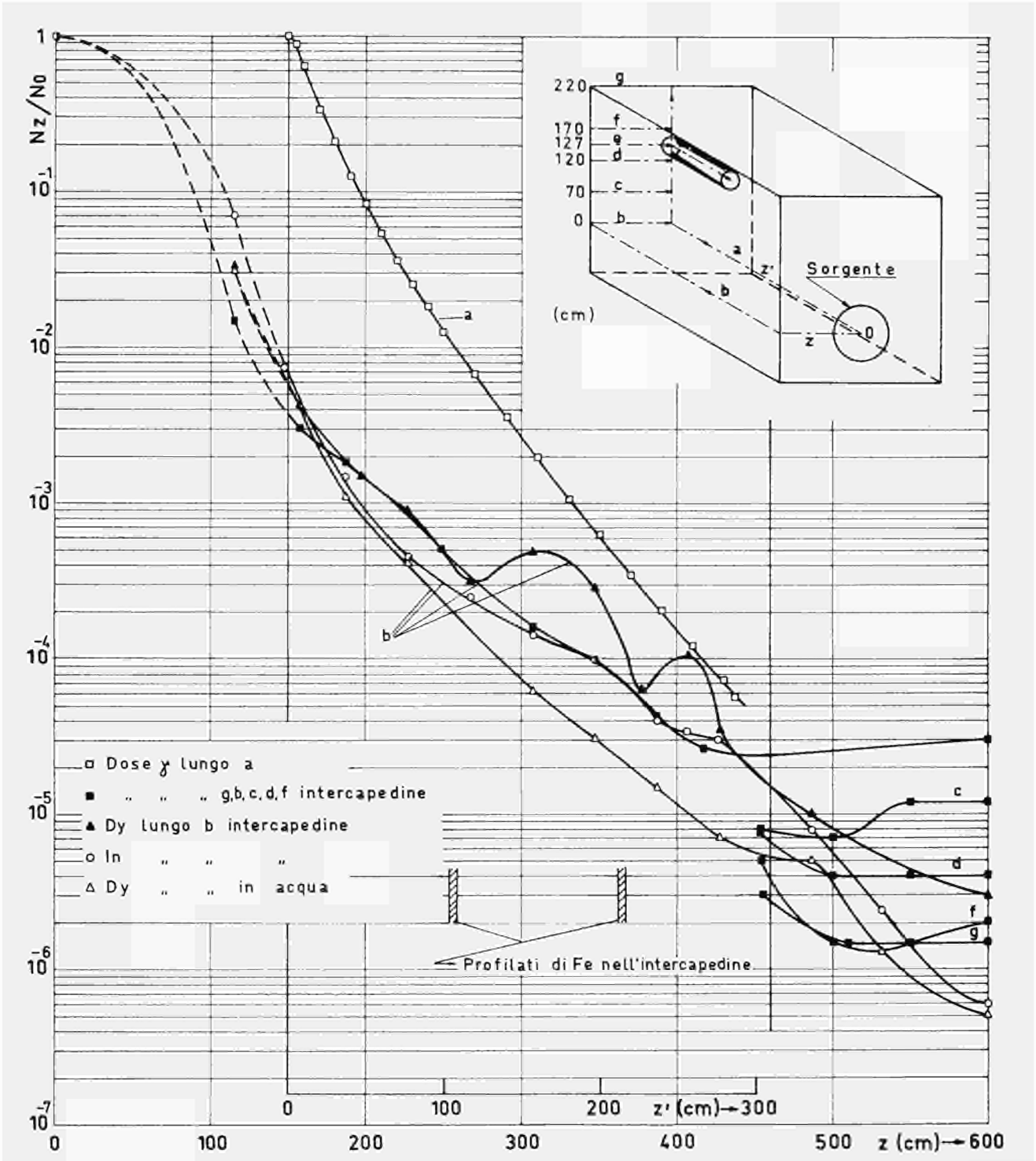

Fig. 13 - Thermal and epithermal reaction rates and γ doses along lines a (water) and b to g (gap around the tank): squares: γ doses (open a, full b to f); triangles: thermal (open b in the gap, full b in water 3 cm from the Al wall); circles: epithermal (b)

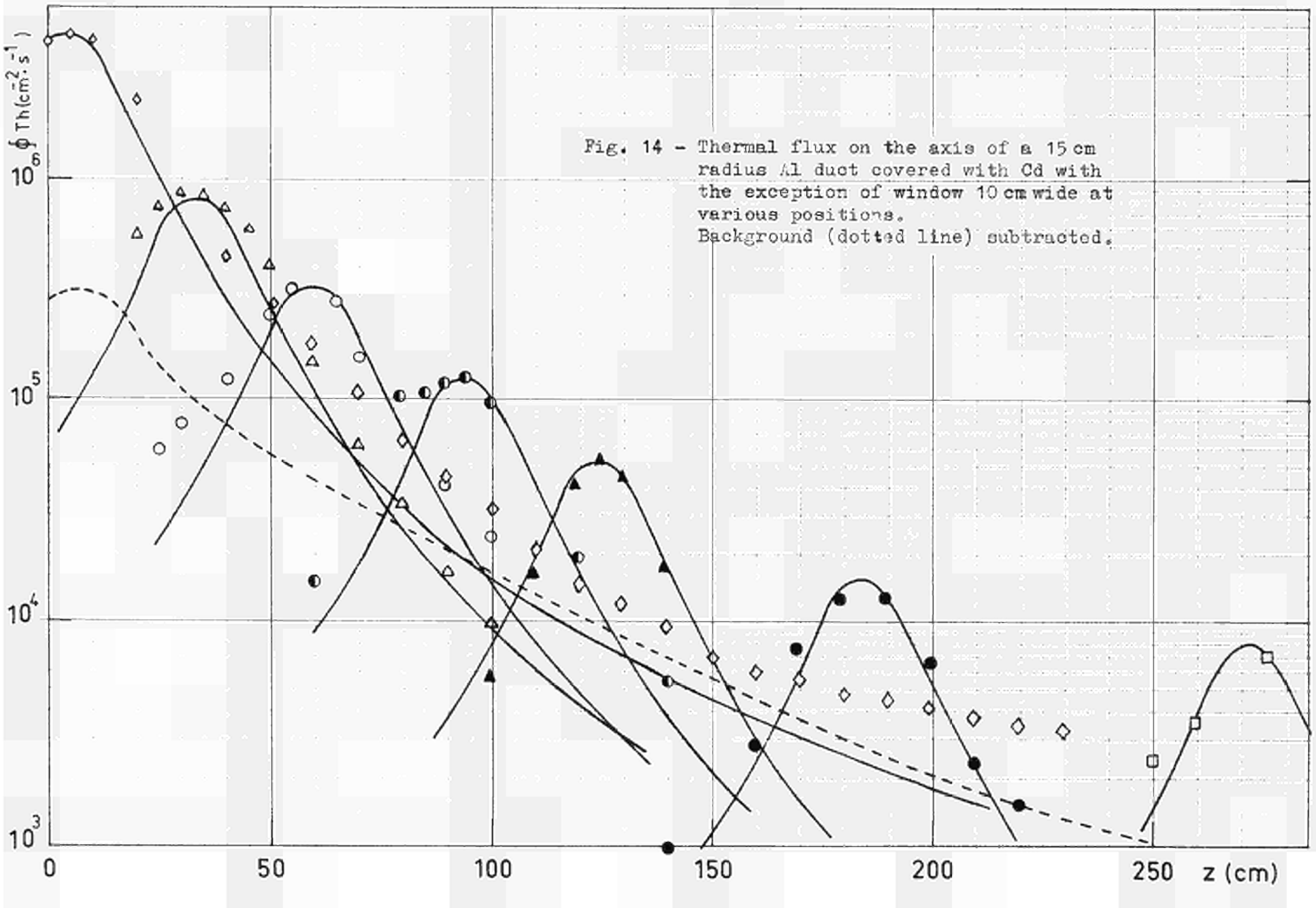

Fig. 14 - Thermal flux on the axis of a 15 cm radius Al duct covered with Cd with the exception of window 10 cm wide at various positions.
Background (dotted line) subtracted.

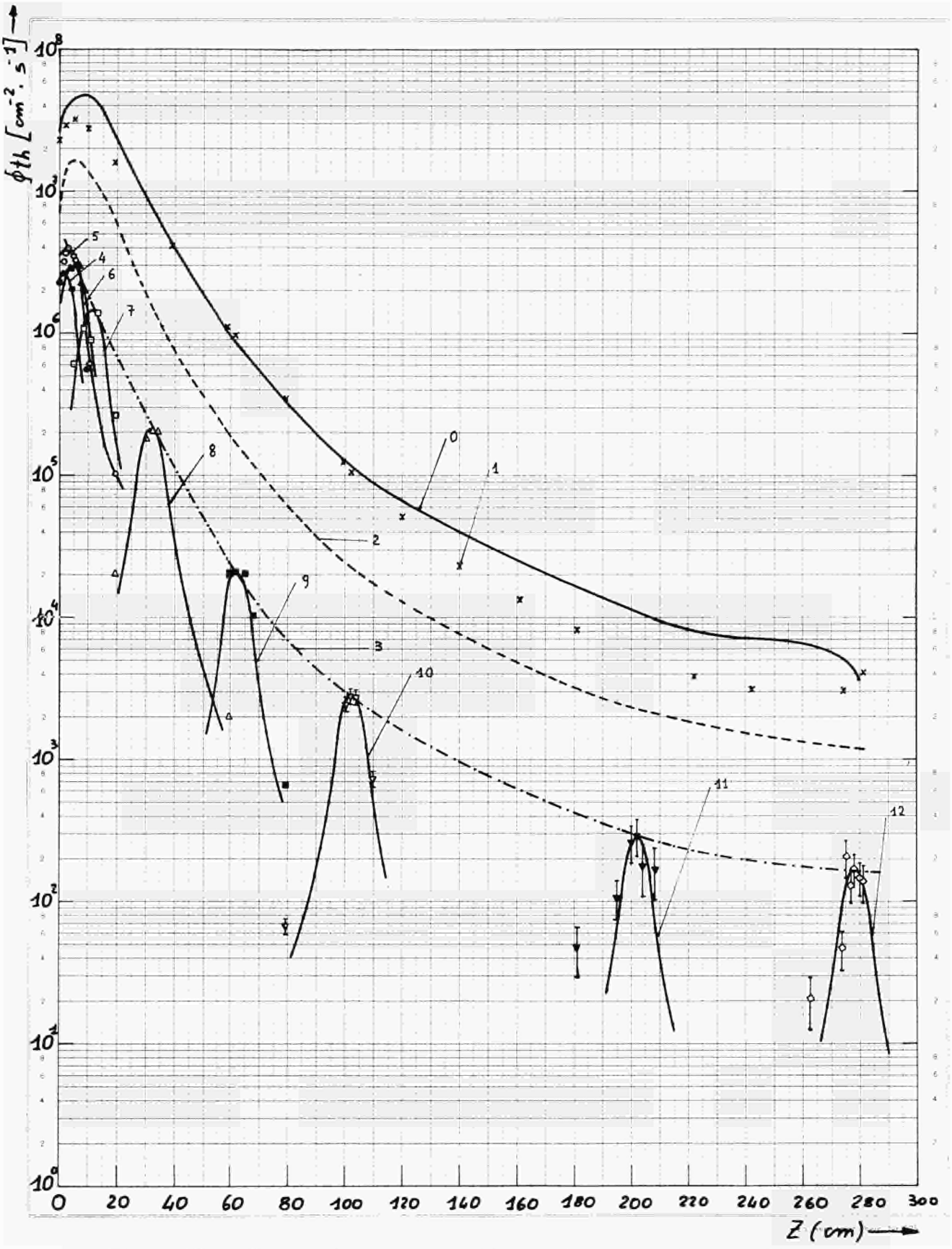

Fig. 15 - Thermal flux on the axis of a 5 cm radius Al duct: 1 bare duct
4 ÷ 7 Cd covered, window 2 cm wide
8 ÷ 12 Cd covered, window 4 cm wide
Background subtracted.

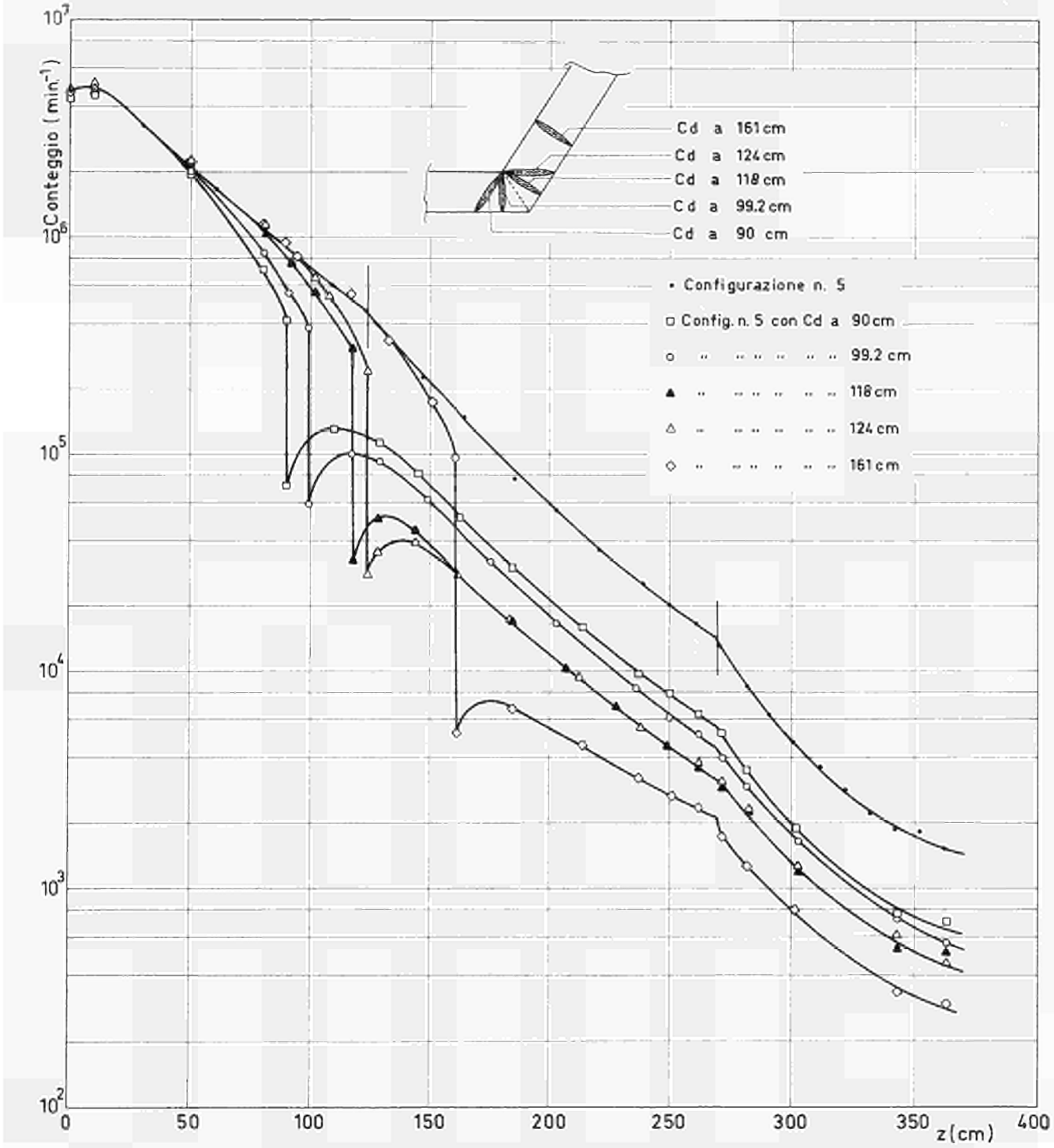

Fig. 16 - Dy counting rate along the axis of configuration 5 showing the effect of a Cd shutter put in warious positions along the duct. To convert in thermal flux multiply by 4.9.

NOTICE TO THE READER

All scientific and technical reports are announced, as and when they are issued, in the monthly periodical **"euro abstracts"**, edited by the Centre for Information and Documentation (CID). For subscription (1 year : US$ 16.40, £ 6.17, BF 820) or free specimen copies please write to :

Handelsblatt GmbH
"euro abstracts"
Postfach 1102
D 4 Düsseldorf 1 (Deutschland)

or

Office de vente des publications officielles
des Communautés européennes
37, rue Glesener
Luxembourg

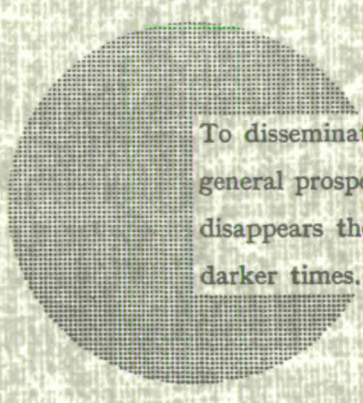

To disseminate knowledge is to disseminate prosperity — I mean general prosperity and not individual riches — and with prosperity disappears the greater part of the evil which is our heritage from darker times.

Alfred Nobel

SALES OFFICES

All reports published by the Commission of the European Communities are on sale at the offices listed below, at the prices given on the back of the front cover. When ordering, specify clearly the EUR number and the title of the report which are shown on the front cover.

SALES OFFICE FOR OFFICIAL PUBLICATIONS OF THE EUROPEAN COMMUNITIES

37, rue Glesener, Luxembourg (Compte chèque postal N° 191-90)

BELGIQUE — BELGIË
MONITEUR BELGE
rue de Louvain 40-42 - 1000 Bruxelles
BELGISCH STAATSBLAD
Leuvenseweg 40-42 - 1000 Brussel

DEUTSCHLAND
BUNDESANZEIGER
Postfach - 5000 Köln 1

FRANCE
SERVICE DE VENTE EN FRANCE
DES PUBLICATIONS DES
COMMUNAUTES EUROPEENNES
26, rue Desaix - 75 Paris 15e

ITALIA
LIBRERIA DELLO STATO
Piazza G. Verdi, 10 - 00198 Roma

LUXEMBOURG
OFFICE DE VENTE
DES PUBLICATIONS OFFICIELLES
DES COMMUNAUTES EUROPEENNES
37, rue Glesener - Luxembourg

NEDERLAND
STAATSDRUKKERIJ
Christoffel Plantijnstraat - Den Haag

UNITED KINGDOM
H. M. STATIONERY OFFICE
P.O. Box 569 - London S.E.1

Commission of the
European Communities
D.G. XIII - C.I.D.
29, rue Aldringer
Luxembourg